J Neurophysiol 108: 2867–2883, 2012.
First published September 5, 2012; doi:10.1152/jn.00312.2012.

Relationships between neck muscle electromyography and three-dimensional head kinematics during centrally induced torsional head perturbations

Farshad Farshadmanesh,[1,2] Patrick Byrne,[1,2] Hongying Wang,[1,2] Brian D. Corneil,[2,3] and J. Douglas Crawford[1,2]

[1]*York Center for Vision Research, Departments of Psychology, Biology, and Kinesiology and Health Sciences, York University, Toronto, Ontario, Canada;* [2]*The Canadian Action and Perception Network (CAPnet), Toronto, Ontario, Canada;* [3]*Departments of Physiology and Pharmacology and Psychology, University of Western Ontario, London, Ontario, Canada*

Submitted 12 April 2012; accepted in final form 29 August 2012

Farshadmanesh F, Byrne P, Wang H, Corneil BD, Crawford JD. Relationships between neck muscle electromyography and three-dimensional head kinematics during centrally induced torsional head perturbations. *J Neurophysiol* 108: 2867–2883, 2012. First published September 5, 2012; doi:10.1152/jn.00312.2012.—The relationship between neck muscle electromyography (EMG) and torsional head rotation (about the nasooccipital axis) is difficult to assess during normal gaze behaviors with the head upright. Here, we induced acute head tilts similar to cervical dystonia (torticollis) in two monkeys by electrically stimulating 20 interstitial nucleus of Cajal (INC) sites or inactivating 19 INC sites by injection of muscimol. Animals engaged in a simple gaze fixation task while we recorded three-dimensional head kinematics and intramuscular EMG from six bilateral neck muscle pairs. We used a cross-validation-based stepwise regression to quantitatively examine the relationships between neck EMG and torsional head kinematics under three conditions: *1*) unilateral INC stimulation (where the head rotated torsionally toward the side of stimulation); *2*) corrective poststimulation movements (where the head returned toward upright); and *3*) unilateral INC inactivation (where the head tilted toward the opposite side of inactivation). Our cross-validated results of corrective movements were slightly better than those obtained during unperturbed gaze movements and showed many more torsional terms, mostly related to velocity, although some orientation and acceleration terms were retained. In addition, several simplifying principles were identified. First, bilateral muscle pairs showed similar, but opposite EMG-torsional coupling terms, i.e., a change in torsional kinematics was associated with increased muscle activity on one side and decreased activity on the other side. s, whenever torsional terms were retained in a given muscle, they were independent of the inputs we tested, i.e., INC stimulation vs. corrective motion vs. INC inactivation, and left vs. right INC data. These findings suggest that, despite the complexity of the head-neck system, the brain can use a single, bilaterally coupled inverse model for torsional head control that is valid across different behaviors and movement directions. Combined with our previous data, these new data provide the terms for a more complete three-dimensional model of EMG: head rotation coupling for the muscles and gaze behaviors that we recorded.

interstitial nucleus of Cajal; neck muscles electromyography; head kinematics; cross-validation; cervical dystonia; torticollis

THE NEUROMUSCULAR CONTROL of three-dimensional (3D) head orientation [horizontal (yaw), vertical (pitch), and torsional (roll)] is important in several aspects of sensorimotor neuroscience. Head torsion (about the nasooccipital axis, also called roll) alters the spatial orientation of the eyes, ears, and vestibular apparatus and therefore has a profound influence on the perceptual function of these sensory organs (Angelaki and Dickman 2003; Blohm et al. 2008; Medendorp et al. 2002). Head torsion also alters the spatial relationship between these sensory organs and alters the sensorimotor transformations originating from these sensors (Blohm and Crawford 2007; Klier and Crawford 1998; Ren and Crawford 2009). For these and other reasons, during gaze behaviors the head is normally maintained upright with torsion constrained within a narrow range of approximately ±5° (Straumann et al. 1991; Tweed 1992), specifically around the torsional axis provided in Fick coordinates (Ceylan et al. 2000; Crawford et al. 1999; Glenn and Vilis 1992; Radau et al. 1994). This "Fick Constraint" has thus been described as an optimal solution to the degrees of freedom problem in head control (Crawford et al. 2011; Crawford et al. 2003). However, certain clinical conditions result in torticollis ("twisted neck") where the head is no longer upright, but rather shows specific torsional offsets (Chan et al. 1991; Malouin and Bedard 1982; Medendorp et al. 1999).

A complete understanding of 3D head posture and movement control requires knowledge of the relative contributions of muscles, like that approached in the oculomotor system (Demer et al. 2000; Robinson 1975; Simpson and Graf 1981). However, the complexity and redundancy of the head-neck system make this a nontrivial problem. Several theoretical and experimental studies have attempted to examine the quantitative relations between neck muscle activation and head kinematics, but fundamental questions of neuromuscular control remain that can only be answered with a better knowledge of the head-neck system (Corneil et al. 2002b; Farshadmanesh et al. 2008; Peterson et al. 2001; Siegmund et al. 2007).

Unfortunately, the redundant configuration of the neck musculature (Peterson and Richmond 1988; Richmond et al. 2001; Richmond and Vidal 1998) does not allow for a direct correlation between anatomical configuration of a neck muscle and its functional role. In a previous study (Farshadmanesh et al. 2012), we attempted to overcome these hurdles by employing a conservative cross-validation-based stepwise regression procedure, designed to establish the relationships between intramuscular neck electromyography (EMG) and head kinematics during natural gaze behavior in monkeys. This allowed us to establish the relationships between EMG activation in 12 neck muscles (six pairs) in the monkey and the horizontal and vertical aspects of head orientation and rotation. However, we were unable to correlate neck EMG to torsional head posture

Address for reprint requests and other correspondence: J. D. Crawford, Center for Vision Research, Computer Science and Engineering Bldg., York Univ., 4700 Keele St., Toronto, Ontario, Canada M3J 1P3 (e-mail: jdc@yorku.ca).

and obtained only a few terms for torsional rotation during head movements. These findings, however, were likely limited by the small variance of torsional motion and position in natural gaze shifts.

It is unclear how one might train monkeys to evoke torsional head movements without rotating the entire body, but another way to overcome such limitations is to directly evoke head torsion through neural perturbations. The interstitial nucleus of Cajal (INC) is thought to control torsional and vertical head posture (Fukushima 1987; Klier and Crawford 2003; Klier et al. 2002). In monkeys and cats, unilateral stimulation of the INC evokes torsional (i.e., relative to a nasooccipital axis) head rotations. Left INC stimulation evokes counterclockwise (CCW) head rotations, whereas clockwise (CW) rotations (from animal's view point) are observed during right INC stimulation (Farshadmanesh et al. 2007; Fukushima et al. 1985; Klier et al. 2002). Moreover, these deviations in head torsion are generally corrected during the next gaze shift that follows stimulation (Klier et al. 2007), presumably through the activation of endogenous circuits similar to those used to correct eye torsion (Van Opstal et al. 1996). Finally, unilateral inactivation of the INC produces torsional head tilts in the direction opposite to that observed during stimulation (Klier et al. 2002; Klier et al. 2007). In a previous paper (Farshadmanesh et al. 2008), our laboratory compared neck muscle recruitment during INC stimulation with that following INC inactivation. Although we observed straightforward patterns of comparative recruitment on some neck muscles (i.e., increased/decreased recruitment following INC stimulation/inactivation), this was not observed in all muscles, potentially because of adaptive or compensatory mechanisms engaged during INC inactivation. Moreover, in our study INC inactivation did not always lead to muscle relaxation. It caused an increase in the activity of some muscles and a decrease in others [see (Farshadmanesh et al. 2008) for details]. However, this study did not control for different distributions of head kinematics (orientation, velocity, or acceleration) following stimulation and inactivation and also compared muscle recruitment during stimulation-evoked movements to that following inactivation-evoked postures. Moreover, that study only compared EMG levels between similar torsional postures; we were not yet able to directly calculate EMG-kinematic coupling terms.

The tilted head posture observed following unilateral INC inactivation in monkeys is also clinically significant as an experimental model for a form of torticollis in humans known as cervical dystonia (Loher et al. 2004). Other studies have also suggested a causal relationship between INC dysfunction and torticollis (Farshadmanesh et al. 2007; Malouin and Bedard 1982; Munchau and Bronstein 2001; Vasin et al. 1985). Moreover, neck muscle EMG has been proven to be useful during the diagnosis (Vasilescu and Dieckmann 1975) and treatment follow-up (Domzal and Tutaj 2000) of torticollis. As an experimental model to study the underlying neural mechanism of torticollis, INC stimulation examines the potential inappropriate upstream inputs to the INC (e.g., from the basal ganglia) (Farshadmanesh et al. 2007; Klier et al. 2002), whereas INC inactivation can be used to assess the effect of direct damage to the INC (Klier et al. 2002; Klier et al. 2007). Thus, by a comparison of EMG-kinematic relations during these two types of INC perturbation, our results could aid in understanding the neuromuscular basis for torticollis and provide insight into brain stem control of neck muscle activation.

The goal of the present study was to combine the approaches of our laboratory's two previous studies on neck EMG during INC perturbation (Farshadmanesh et al. 2008) and cross-validated models of EMG-kinematic coupling (Farshadmanesh et al. 2012), which both employed the same animals and EMG preparation, to determine the coupling between neck muscle EMG and torsional head kinematics in the monkey. Taken together with our laboratory's previous study (Farshadmanesh et al. 2012), this would provide a more complete 3D model of EMG coupling to rotational head kinematics in the monkey, within the muscles and gaze behaviors that we studied. Here, we tested the relationship between neck EMG (in six bilateral neck muscle pairs) and head kinematics during head movements that *1*) were evoked by INC stimulation; *2*) returned the head toward center (corrective or returning head movements); and *3*) were elicited voluntarily after INC inactivation. We took advantage of the fact in each of these data sets, as we shall demonstrate in the RESULTS section, that there are different but still considerable ranges of torsional head orientation, velocities, and accelerations, even after INC inactivation (Farshadmanesh et al. 2007). Among data sets, the corrective head movements were arguably closest to those observed during natural gaze behavior because they were not directly evoked by INC stimulation or elicited during tilted head orientations caused by INC inactivation, whereas the other data sets were most relevant as an animal model for torticollis [both INC stimulation and inactivation are shown to evoke torticollis-like head tilts (Klier et al. 2002)].

Our specific aims were to *1*) complete our 3D model for EMG-kinematic coupling (Farshadmanesh et al. 2012) by adding in torsional terms for the individual muscles in the six pairs we tested; *2*) test several basic assumptions about synergy and symmetry, i.e., between left and right muscles of a pair and left and right INCs; *3*) determine whether different methods of torsional perturbation directly influence EMG-kinematic coupling, or only through the ranges of head kinematics distribution they produce; and *4*) ultimately use these data to understand the neuromuscular coupling in the head-neck system in physiological and pathological situations.

METHODS

The general surgical, experimental, and analytic procedures for this series of experiments have been reported previously (Farshadmanesh et al. 2007; Farshadmanesh et al. 2008), as well as our cross-validation analytic method (Farshadmanesh et al. 2012), applied previously during natural gaze behavior, but applied here to head movements that include torsional perturbations. Here we summarize the essential methods, along with any analytic methodologies specific to this study.

Surgical Procedures

All surgical protocols were in accordance with the Canadian Council on Animal Care guidelines on the use of laboratory animals and were preapproved by the York University Animal Care Committee.

Eye and head search coils. An acrylic skull-cap was implanted in two female *Macaca mulatta* monkeys (M1 and M2) as a base for our recording attachments and a quick-release head restraint. A stainless steel recording chamber was implanted above stereotaxic coordinates

of five anterior and zero lateral for access to the INC. Two eye coils were implanted in one eye of each animal for training and our gaze control paradigms.

EMG electrodes. Two weeks after the first surgery, we implanted chronically indwelling bipolar hook electrodes (stainless steel, Teflon-coated AS631 Cooner Wire) in the following six bilateral neck muscle pairs (see Elsley et al. 2007 for details): sternocleidomastoid (SCM), splenius capitis (SP), rectus capitis posterior major (RCPmaj), occipital capitis inferior (OCI), biventer cervicis (BC), and complexus (COM). The wires of the electrodes were connected to a connector embedded within the acrylic skull-cap. These muscles are all expected to contribute to either ipsilateral or contralateral head tilt (Corneil et al. 2001; Richmond et al. 2001).

Experimental Task

The purpose of this task (same task as in Farshadmanesh et al. 2012) was to encourage visual fixation (and more importantly, a natural dispersion of head orientations) over a broad 3D range. In a dark room, the animals were first required to fixate a white cross that was back-projected at the center of a black screen in front of them. Animals were trained to fixate one of nine peripheral targets that appeared as white dots in a random order within a 60° × 60° grid on a black screen (one center; four up, down, left, and right, each 30° from center; four in between, each 42° from center, see Fig. 1*B* in Farshadmanesh et al. 2012 for an overview). A juice reward was delivered when *1*) the animal fixated a target for a minimum of 500 ms; and *2*) the animal's gaze and head orientations were within computer-controlled visual fixation windows (around every target; gaze, 10° diameter; head, 20° diameter; similar for INC stimulation, corrective movement, and INC inactivation conditions); and *3*) when the head speed was ≤10°/s. Each target remained visible for 6–10 s before extinguishing (to encourage stable eye and head postures), and then a new target was presented on the screen. Other than the perturbations described below, animals were allowed to move their heads freely, in a matter of their own choice, at all times during this task. Overall, except for torsion, the obtained horizontal (left-right) [INC stimulation (M1, 88°-98°, M2, 99°-97°); INC inactivation (M1, 84°-90°, M2, 91°-103°)] and vertical (down-up) [INC stimulation (M1, 31°-77°, M2, 24°-45°); INC inactivation (M1, 30°-75°, M2, 26°-53°)] range were similar to those in our laboratory's previous study [horizontal (M1, 92°-96°; M2, 97°-105°) and vertical (M1, 30°-73°; M2, 28°-49°)] (Farshadmanesh et al. 2012).

INC Stimulation and Inactivation

At the beginning of each experiment session, we selected a potential INC location along anterioposterior and mediolateral coordinates using a method described previously (Farshadmanesh et al. 2007). Each preselected location was electrically stimulated at different vertical depths (sites) with minimum separation of 500 μm using 50-μA monophasic cathodal pulses with pulse widths of 0.5 ms, frequency of 300 Hz, and pulse trains of 200 ms (Klier et al. 2007). The stimulation pulse was delivered 1,000 ms after the monkey's gaze and head entered the fixation window during the task. For each INC site, we ran at least one block of the task and delivered stimulation randomly three times for each target location within the block (i.e., at least 27 stimulation pulses were delivered for each INC site). In total, five (M1) and five (M2) sites were stimulated in the left INC, and five (M1) and five (M2) in the right INC. For each site, a range of 41 ± 9.3 (mean ± SD) movements were evoked by stimulation.

For inactivation trials, we injected 0.3 μl of 0.05% muscimol solution into the upper and lateral region of the INC site where stimulation evoked the largest head rotation for that particular INC location (Farshadmanesh et al. 2007). Data were recorded for a minimum of 40 min after injection, while the monkey continued to perform the task. Experimental sessions were conducted every other day to allow enough time for recovery from a performed injection. We confirmed the locations of the injections by postmortem histological analysis (Farshadmanesh et al. 2007; Klier et al. 2007). A total of four (M1) and seven (M2) injections were done in the left INC, and four (M1) and four (M2) in the right INC. In this study, we only describe data from sites that were explored using both stimulation and inactivation.

Data Collection

Before each experiment session, a plastic platform containing two orthogonal 3D coils was attached to the skull cap for recording instantaneous head orientation (Crawford et al. 1999). Eye and head coil signals were digitized at a 10-kHz sampling rate and then downsampled offline by a factor of 10 to 1 kHz. We then calculated eye and head quaternions, which represent the orientations of the eye and head relative to a central reference orientation in Cartesian coordinates embedded within the stationary laboratory frame, from these coil signals (Crawford et al. 1999; Farshadmanesh et al. 2007; Tweed et al. 1990). These were then transformed into other coordinates, velocity, and acceleration (i.e., head orientation time derivatives) as required. Unless stated otherwise, the data shown in this paper provide head orientation and its time derivatives in "Fick coordinates", where the torsional axis is embedded on a head-fixed horizontal axis (i.e., nasooccipital axis), which in turn rotates around a space-fixed vertical axis (Glenn and Vilis 1992). Recorded EMG signals were first differentially amplified at a head stage that was plugged directly into the EMG connector (×20 gain), bandpass filtered (20 Hz to 17 kHz), and finally were fed into a signal processing unit (Plexon, ×50 gain; bandwidth, 100 Hz to 4 kHz) to be digitized at 10 kHz for later offline analysis.

Data Selection

We first rectified EMG data and then integrated them into 1-ms time bins (Bak and Loeb 1979; Corneil et al. 2001). We further divided our data into 10-ms time bins (which still include the lowest frequency of our EMG signals at 300–3,000 Hz) for offline analysis (Farshadmanesh et al. 2012). We then selected the head movement intervals during the three examined conditions (INC stimulation, corrective movements, and INC inactivation) as described below (See Fig. 1 for the windows used for data selection).

INC stimulation. Left INC stimulation always evoked CCW head rotations (see Fig. 2*B*), whereas right INC stimulation always produced CW rotations (Farshadmanesh et al. 2008; Farshadmanesh et al. 2007; Klier et al. 2002). We analyzed 278 (M1) and 336 (M2) such movements evoked by left INC stimulation and 279 (M1) and 232 (M2) by right INC stimulation. The stimulation onset was chosen as the beginning of the stimulation-evoked movement, whereas the "end" of the movement was selected where head speed dropped below 10°/s. Data selection was performed using a custom-built algorithm developed for MATLAB (The MathWorks). Then head orientation, first and second time derivatives of head orientation, and the mean level of EMG activity for every muscle were calculated for the first 10–30 ms of poststimulation period (see Farshadmanesh et al. 2008). This range is likely to involve activation produced by direct interstitio-spinal tract connections and therefore should represent direct phasic effect of INC stimulation and correlate more closely with the acceleration phase of the evoked head movement which we study here. The head speed was >10°/s for all of the selected data in both subjects. To determine the neuromuscular lag between EMG signal and evoked head movement, head orientation, first and second time derivatives of head orientation of up to 100 ms after the end of the selected point (110–130 ms) were included in the analysis (see Farshadmanesh et al. 2012 for details on determining the neuromuscular lag).

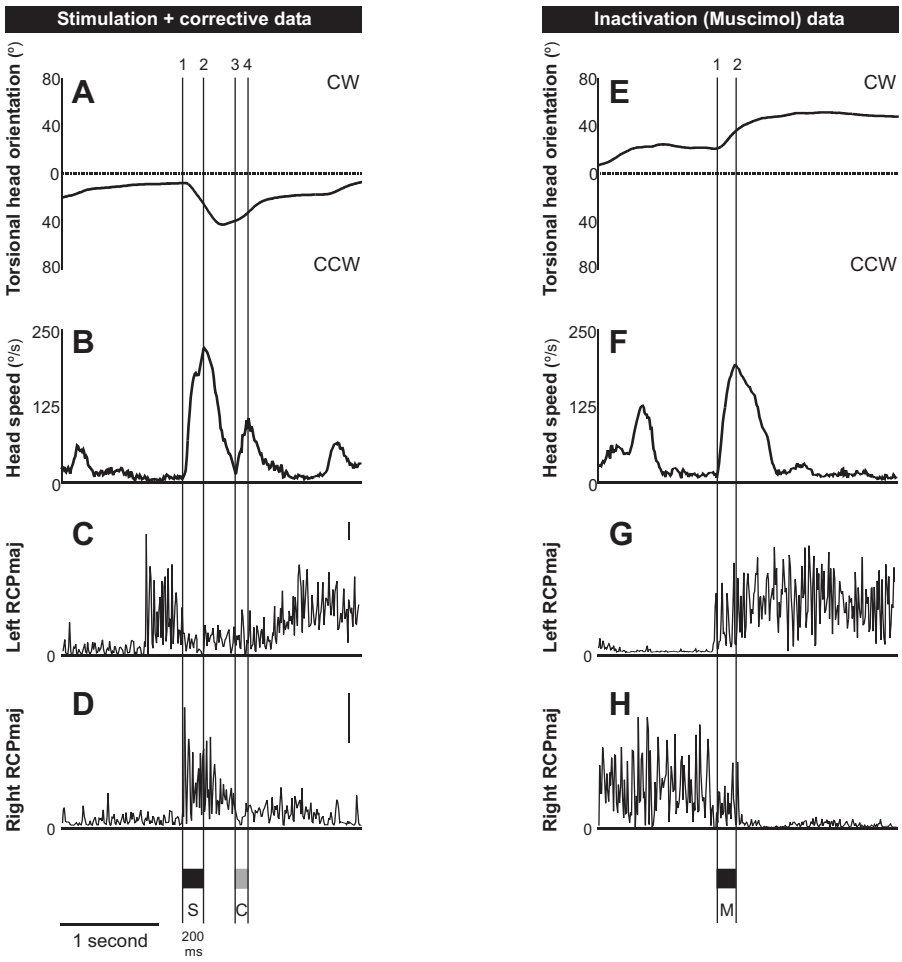

Fig. 1. Data selection. Torsional head orientation (*A* and *E*), head speed (*B* and *F*), and examples of EMG activity for left (*C* and *G*) and right (*D* and *H*) rectus capitis posterior major (RCPmaj) muscles for left interstitial nucleus of Cajal (INC) stimulation, a corrective movement (*left* column), and left INC inactivation (*right* column). For stimulation data (marked S in the *bottom*), head orientation and its time-derivatives (i.e., head velocity and head acceleration), together with muscle EMG, were calculated during the first 10–30 ms of the stimulation interval (marked automatically, seen in the *left* column, between vertical *lines 1* and *2*), which, as seen in head speed trace (*B*), is comparable to the acceleration phase of the evoked movement. For corrective movement data (marked C in the *bottom*), each movement was marked manually, and then a random point within the acceleration phase (between vertical *lines 3* and *4*) was selected so that it was at least 150 ms apart from stimulation offset (see METHODS). For inactivation (muscimol) data (*right* column, marked M in the *bottom*), head was considered moving where its speed was larger than 10°/s. A random point within the acceleration phase of each and every movement (here, between vertical *lines 1* and *2* in the *right* column) was chosen to calculate head orientation, its time-derivatives, and neck EMG. To account for the neuromuscular delay, for stimulation data, the EMG activity of up to 100 ms after the selected 10- to 30-ms range (i.e., 110–130 ms) was included in the fitting process for each selected movement. For corrective movements and inactivation data, the EMG activity of up to 100 ms prior to the selected point was included in the analysis so that, for corrective movement data, it was at least 50 ms apart from the stimulation offset (see METHODS). Vertical scale bars on the *right* of EMG panels *C* (same for *G*) and *D* (same for *H*) denote 100 μV. Data are from *animal M2*. CW, clockwise; CCW, counterclockwise.

Corrective movements. Gaze shifts and head movements that follow immediately after INC microstimulation include torsional components that bring the eye and head back toward their normal orientation range (see Fig. 2*C*) (Crawford 1998; Klier et al. 2006). These appear to be endogenously generated corrective movements (Van Opstal et al. 1996). Here, we used these movements to represent the most naturally generated torsion (compared with stimulation-evoked movements and inactivation-related perturbations). We analyzed 275 (M1) and 292 (M2) such movements following stimulation of the left INC and 273 (M1) and 224 (M2) following stimulation of the right INC.

The beginning of each corrective movement was marked manually (to confirm the prior, stimulation-evoked movement was finished) when the preceding stimulation-evoked movement was complete, whereas its end was selected automatically where head speed dropped below 10°/s. We followed a procedure similar to that in our laboratory's previous study (Farshadmanesh et al. 2012) to select a random point (to sample more of the EMG-head kinematics relationships) within the acceleration phase (i.e., where magnitude of head acceleration went above 20°/s^2 for more than one 10-ms bin in a row until where head velocity reached its maximum) of each marked corrective movement so that it was at least 150 ms after the stimulation offset (see Farshadmanesh et al. 2012). Because we needed to include EMG activity of up to 100 ms before the selected random point to determine the neuromuscular lag (Farshadmanesh et al. 2012), the latter criterion provided at least 50-ms separation between stimulation offset and the selected corrective movement data.

INC inactivation. Unilateral inactivation of the INC produced torsional head tilts in the direction opposite to that observed during stimulation of the same side (see Fig. 2*D*) (Farshadmanesh et al. 2008; Klier et al. 2002). As in our laboratory's previous study (Farshadmanesh et al. 2008), we analyzed the late phase of INC inactivation (i.e., 40 min of postinjection). We chose this interval because head tilts were relatively stable (i.e., head posture was static) at this time and showed a similar (but opposite) magnitude to head tilts evoked by stimulation of the same INC sites. During the early phase of INC inactivation (i.e., 15 min of postinjection), we often observed drifting movements of the head while head torsion began to show a gradual offset (i.e., tilt), which became largest during the late phase of inactivation and lasted for 8–9 h (Farshadmanesh et al. 2007). The movement intervals during INC inactivation were marked automatically. To obtain head kinematics, within the acceleration phase of the marked movement, a random point was selected with EMG activity of up to 100 ms before the selected random point included in the analysis for neuromuscular lag. The details were similar to our procedure of selecting behavior data published elsewhere (see Farshadmanesh et al. 2012). This resulted in 888 (M1) and 890 (M2) data points from left INC inactivation and 686 (M1) and 643 (M2) data points from right INC inactivation. To exclude any head movements which included head drifts (evoked by the inactivation of the INC and defined by exponential, position-dependent decays in head orientation, see Farshadmanesh et al. 2007 for details), the marked inactivation data were inspected manually, and 48 out of 1,574 movements in M1 (3.05%) and 110 out of 1,533 movements in M2 (7.18%) were removed from the pool.

Data Analysis: Cross-Validation and Stepwise Regression

The purpose of our analysis was to derive the simplest polynomial model capable of capturing the underlying relationship between neck

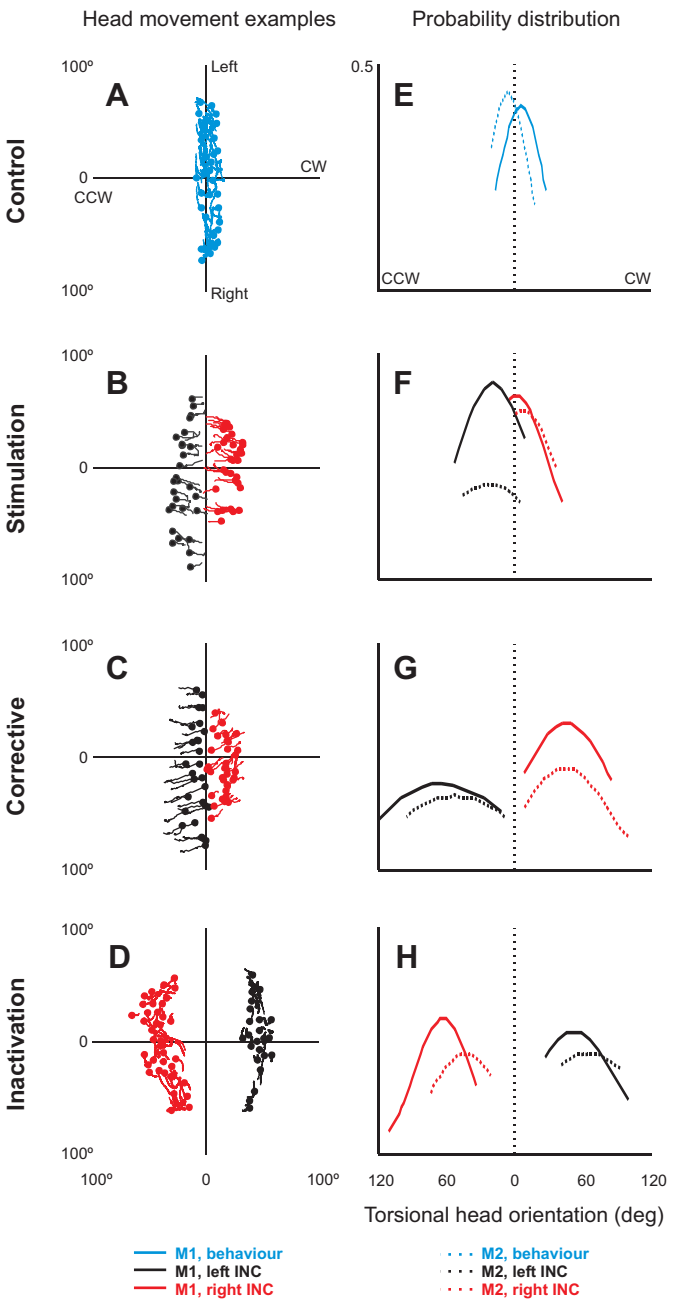

Fig. 2. Overview of head movements. Examples of head movements are shown as horizontal vs. torsional head orientation (*left* column) for *animal M2*. *Rows 1–4* represent control (*A*), INC stimulation (*B*), corrective movement (*C*), and INC inactivation (*D*) data. Blue color indicates behavioral data, whereas black and red represent left and right INC data, respectively. *Right* column (*E*, *F*, *G*, and *H*) shows the probability distributions of all torsional head orientation at the beginning of every movement for *animals M1* (solid lines) and *M2* (dotted lines). The curve ends are truncated according to the range of data.

muscle EMG and head kinematics. The method employed to accomplish this has been described in detail elsewhere (Farshadmanesh et al. 2012). Essentially, we performed a stepwise regression in which a cross-validation-based measure of model generalizability was used for term selection. In particular, we divided each of our six data sets (two for left/right INC stimulation, two for corrective movements during left/right INC stimulation, and two for left/right INC inactivation) into 10 equal-sized folds each. We then took the horizontal and vertical orientation term coefficients we obtained for each muscle from our laboratory's previous behavioral study (Farshadmanesh et al. 2012) and added torsional orientation (T, T^2, T^3, T^4), torsional velocity ($\dot{T}$, $\dot{T}^2$), torsional acceleration ($\ddot{T}$, $\ddot{T}^2$), and the interaction terms (between torsional orientation and torsional velocity/acceleration, $\dot{T}T$, $\dot{T}T^2$, $\dot{T}^2T$, $\dot{T}^2T^2$, $\ddot{T}T$, $\ddot{T}T^2$, $\ddot{T}^2T$, $\ddot{T}^2T^2$) to the set of possible terms to be included in the final model. At each step of the stepwise regression procedure, we calculated model generalizability by fitting to nine of the subfolds and calculating the sum of square residuals (R^2_{cv}) on the remaining fold. By repeating this for all combinations of folds, the average value of R^2_{cv} for that model (its generalizability) was determined. Based on this value, the current term was accepted/rejected (see Farshadmanesh et al. 2012 for details).

We simplified the model for each muscle (that was determined via stepwise regression) to determine the model terms that contributed most to the R^2_{cv} by step-by-step removal of the largest possible number of terms that collectively (together) contributed less than 0.05 to the total R^2_{cv} value of the model (see Farshadmanesh et al. 2012). The remaining terms of the simplified models are shown separately for each muscle separate for INC stimulation, corrective movement, and INC inactivation data in Tables 1–4. Because, in our behavioral cross-validation study, we observed as good or marginally better R^2_{cv} in Fick coordinates compared with the other alternatives (e.g., space or head coordinates), we chose Fick angles as our default coordinate system.

RESULTS

Temporal Head Kinematics and Neck EMG

Fig. 1 illustrates the relative timing of head responses and neck EMG, and the windows used to select our three data sets (see METHODS) with the use of typical example trials and muscle recordings. The *left* column of Fig. 1 represents head orientation (Fig. 1*A*), head speed (Fig. 1*B*), and EMG activation of left and right RCPmaj muscles (Fig. 1, *C* and *D*, respectively) during a head movement evoked by stimulating a left INC site and during a subsequent corrective movement in animal M2. In this example, following the stimulation (Fig. 1*A*), head rotated CCW, while the subsequent corrective movement brought the head back toward its initial orientation. The activity of left RCPmaj (Fig. 1*C*) was suppressed after stimulation onset during the corrective movement (with the baseline activity seen before the observed activation up to around 400 ms before stimulation onset). In contrast, INC stimulation evoked an increase in the EMG activity of right RCPmaj (Fig. 1*D*), which returned to its baseline by the end of stimulation-evoked movement. In the *right* column, Fig. 1*E* shows a CW head rotation during inactivation of the same left INC site in the same animal on the same day. Subjects were still able to make head movements in both CW and CCW directions after inactivating either left or right INC, and the observed movements had qualitatively comparable kinematics to those observed during INC stimulation. In this example, the activation of left RCPmaj gradually increased during the acceleration phase of the movement (Fig. 1*G*, between vertical *lines 1* and *2*) simultaneous with a gradual decrease in the EMG activity of right RCPmaj (Fig. 1*H*). These and similar data are quantified thoroughly in the following sections.

Distributions of Head Orientation in the Three Data Sets

In this and the following section, we quantify the distributions of head kinematics used for our cross-validated fits. This was done to establish the range of torsional kinematics of each data set, and to know how to compare their resulting fits. The

left column of Fig. 2 shows example plots of horizontal (left and right rotations about the vertical axis) vs. torsional (CW and CCW rolls about the horizontal axis) head orientation for typical control (*A*), INC stimulation (*B*), corrective movement (*C*), and INC inactivation (*D*) data, all from animal M2.

Control behavioral data are plotted as blue dots, whereas black and red dots show data from perturbation of the left or right INC, respectively. In our control data (Fig. 2*A*), head movements were observed in different random horizontal and vertical (not shown) directions but within a small torsional range. Similar results have been described previously in the human (Ceylan et al. 2000; Glenn and Vilis 1992; Radau et al. 1994) and the monkey (Crawford et al. 1999; Farshadmanesh et al. 2007; Klier et al. 2003; Martinez-Trujillo et al. 2004). This was the type of data used in our previous study and is shown here only for comparison.

Figure 2, *B–D*, illustrates examples of the torsionally perturbed ranges utilized in the present study. INC stimulation (Fig. 2*B*) consistently evoked torsional head movements. Left INC stimulation (black traces) evoked CCW head movements (here, relative to the *y*-axis) toward CCW direction, whereas stimulating the right INC (red traces) caused CW head movements. For each stimulated site, the observed movements had a characteristic amplitude (i.e., here, the length of the traces are similar). Figure 2*C* represents the corrective movements for the same left and right INC sites shown in Fig. 2*B*. These movements returned the head from its poststimulation orientation back toward center and had amplitudes similar to those observed during the stimulation of each corresponding INC site. Inactivation of the same INC site as shown in Fig. 2*B* resulted in a shift in head orientation with a direction opposite to that observed during INC stimulation (CW/CCW after left/right INC inactivation, see Fig. 2*D*). While tilted unilaterally after INC inactivation, the head still moved in different random horizontal and vertical (not shown) directions. Similar results have been described previously for the monkey (Farshadmanesh et al. 2008; Farshadmanesh et al. 2007; Klier et al. 2002).

The *right* column of Fig. 2 quantifies the probability distributions of all torsional head orientations from head acceleration phases used in our laboratory's previous study (Farshadmanesh et al. 2012) (Fig. 2*E*) and in the three data sets used in the current study (Fig. 2, *F–H*). Data are plotted separately for animal M1 (solid lines) and M2 (dotted lines), and for left (black lines) and right (red lines) INC. Note that the curve ends are truncated at the limits of the data range. In the control data, as one would expect, the selected sample distribution was narrow (Fig. 2*E*) and centered around zero torsion (i.e., dotted vertical line). This illustrates why it was difficult to obtain good torsional orientation fits in that study (Farshadmanesh et al. 2012).

For the INC stimulation data set used in the present study (Fig. 2*F*), torsional head orientation distributions were slightly larger but still relatively narrow. This was because our data selection process (see METHODS) chose early motion in the acceleration phase before large amounts of torsion accumulated. Note that here, since evoked head movements began from different initial orientations, there is some overlap between the probability distributions plots. Right INC data showed a slightly shallower range (black vs. red traces). In contrast, torsional orientation distributions from the corrective movement (Fig. 2*G*) and INC inactivation (Fig. 2*H*) data sets from both INCs and both subjects showed much broader, shifted distributions because the acceleration phases of corrective movements started from shifted orientations, and the inactivation data were tonically shifted. Moreover, as expected from the data shown in the *left* column, inactivation data were shifted in opposite directions compared with the other data sets (stimulation and corrective, CCW/CW for left/right INC, inactivation, CW/CCW for left/right INC, respectively). Thus all three of these data sets showed broader torsional orientation ranges than control behavioral data (Fig. 2*E*), but one would expect the corrective and inactivation data sets to provide the best ranges for orientation fitting.

Distributions of Head Velocity in the Three Data Sets

Figure 3 (*left* column) provides typical examples of head velocity (i.e., first time derivative of head orientation) traces. The plots are shown as horizontal vs. torsional head velocity, for control and experimental conditions. Individual velocity traces tend to describe loops, starting near zero, growing to some maximum, and returning toward zero. The probability distributions of torsional head velocity and acceleration (i.e., first and second head orientation time derivatives, respectively) are shown in the *middle* and *right* columns, respectively. Otherwise, the plotting conventions are the same as in Fig. 2.

As seen in Fig. 3*A*, in the control data used for our previous study, head velocity had a smaller torsional distribution compared with the horizontal component. The range of torsional head velocity was much larger for both INC stimulation (Fig. 3*B*) and corrective movement (Fig. 3*C*) data. Left and right INC stimulation evoked CCW and CW head velocities, respectively, whereas, during corrective movements, this was the opposite (i.e., CW/CCW for left/right INC). The range of torsional head velocities was only slightly larger during the 30–40 min of post-INC inactivation (Fig. 3*D*) compared with control data (Fig. 3*A*).

For control data, the range of both first (Fig. 3*E*) and second (Fig. 3*I*) time derivatives were more widely distributed than the corresponding orientation ranges (Fig. 2*E*); this is probably why we were able to obtain some significant torsional motion terms in our laboratory's previous study (Farshadmanesh et al. 2012). Moreover, these were evenly distributed around zero torsion (i.e., dotted vertical line). In contrast, these distribution ranges were shifted in both the INC stimulation (Fig. 3, *F* and *J*) and corrective movement (Fig. 3, *G* and *K*) data sets. The distribution shift was CCW/CW for left/right INC stimulation and CW/CCW for corrective movements. However, first and second time derivative ranges observed in inactivation data (Fig. 3, *H* and *L*, respectively) in both animals were similar to those observed in control data (Fig. 3, *E* and *I*). This was apparently because the orientation ranges had stabilized by 30–40 min after the inactivation, i.e., the torsional corrective movements observed earlier (Klier et al. 2002) had stopped occurring after INC inactivation.

To summarize this and the previous section, as we had hoped, all three of our data sets provided wider ranges of torsional orientation, velocity, and acceleration, overall, compared with the control ranges used in our laboratory's previous study (Farshadmanesh et al. 2012). These ranges were both different and complementary, e.g., the corrective and inactivation data sets showed the largest orientation shifts, whereas the

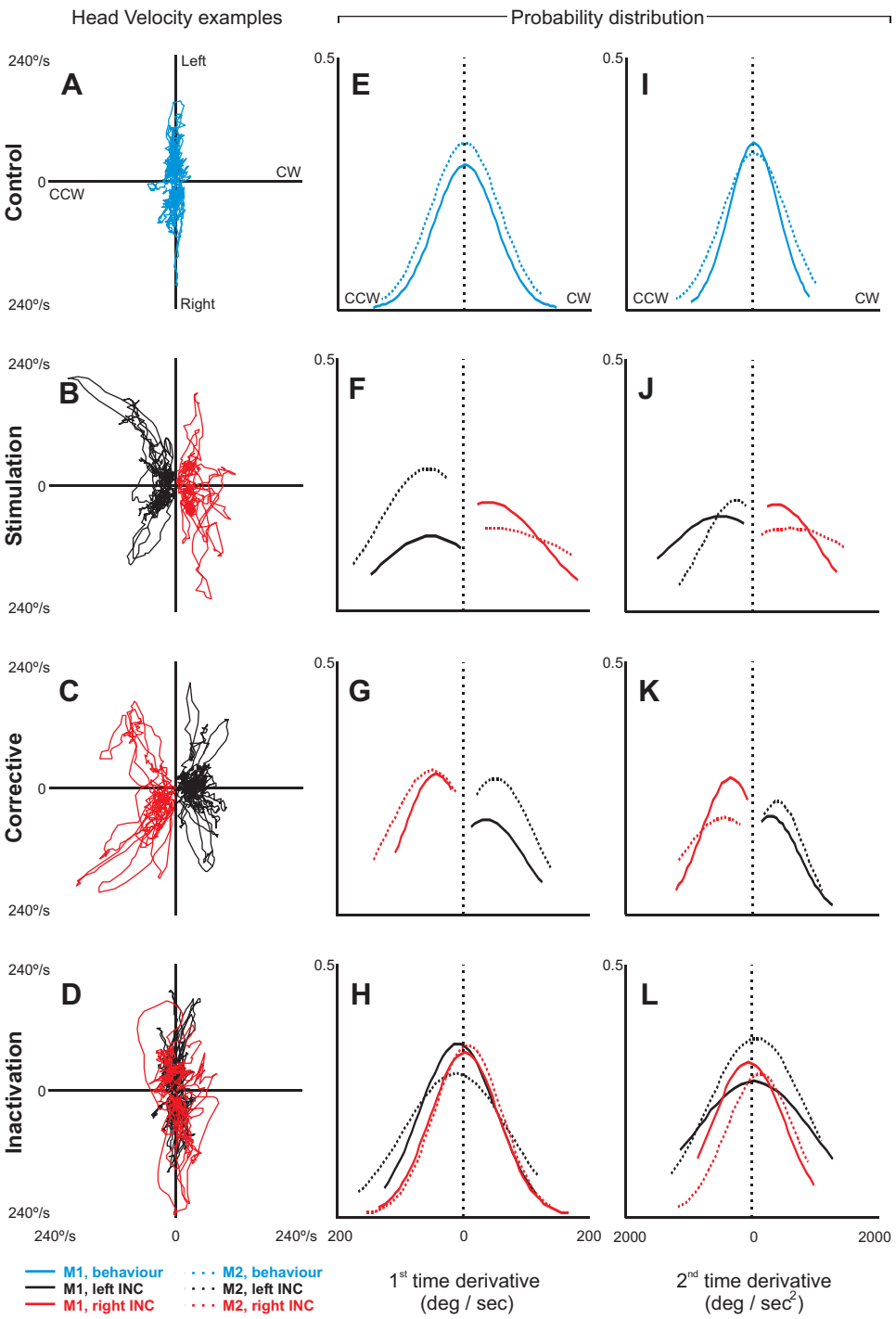

Fig. 3. Overview of head kinematics. Examples of head velocity traces are shown as horizontal vs. torsional head traces (*left* column) for *animal M2*. *Rows 1–4* represent control (*A*), INC stimulation (*B*), corrective movement (*C*), and INC inactivation (*D*) data. Blue color indicates behavioral data, whereas black and red represent left and right INC data, respectively. The probability distributions of first time-derivatives of torsional head orientation (i.e., torsional head velocity) are shown in the *middle* column (*E*, *F*, *G*, *H*), whereas the *right* column (*I*, *J*, *K*, *L*) shows the probability distributions of second time-derivatives (i.e., torsional head acceleration) for *animals M1* (solid lines) and *M2* (dotted lines). The curve ends are truncated according to the range of data.

corrective and stimulation data sets showed the largest velocity and acceleration shifts (and in opposite directions). These factors should be born in mind when we interpret and compare the EMG fits below.

Basic Model for Pooled Corrective Data

Since our corrective data set showed broad shifts in all of the torsional kinematic distributions (see Figs. 2 and 3) and was most likely to correspond to an endogenous physiological signal, we used this data set to evaluate our basic models of torsional head control. To make this data set comparable to that in our study of head movements during normal gaze shifts (where bidirectional movement components were pooled), we first pooled the corrective data recorded following stimulation of both left and right INCs. We then performed our stepwise regression separately for each muscle, as described in METHODS. To examine whether different coordinate representations of head kinematics yield different results (see Farshadmanesh et al. 2012), we ran our regression analysis using both space-fixed Cartesian coordinates and Fick coordinates, which are thought to represent the natural behavioral and mechanical coordinates for the head (Crawford et al. 1999; Glenn and Vilis 1992; Graf

et al. 1995; Richmond and Vidal 1998). Finally, to evaluate the performance of these models, we averaged the R^2_{cv} values across all muscles of each animal.

Overall, the R^2_{cv} results were slightly better than those in our laboratory's analysis on natural gaze shift data (Farshadmanesh et al. 2012) for both animals M1 (0.30 vs. 0.25) and M2 (0.48 vs. 0.36). In other words, even after model simplification (removing less contributing model terms), the model accounted for 30% and 48% of the relationship between the very noisy EMG data and head kinematics in animals M1 and M2, respectively. The R^2_{cv} was higher in animal M1 for Fick (0.30), vs. space (0.26) coordinate representation, but the difference was not significant in either animal (*t*-test, M1, $P = 0.13$; M2, $P = 0.28$). This was inconclusive, but, to be consistent with our laboratory's previous study (Farshadmanesh et al. 2012) and the basic physiology/anatomy of the system, we chose Fick angles as our default coordinate system.

We now describe the actual terms that arose in these models and survived the process of simplification (see METHODS). The terms for both animals are shown in Table 1. While first- and second-order first time-derivative terms ($\dot{T}$, $\dot{T}^2$) were observed in most muscles in both animals, first-order torsional orientation term (T) was only retained in right OCI, right COM of animal M1 and left SCM of animal M2. Similarly, first-order second time-derivative term ($\ddot{T}$) was only observed in left BC of animal M1 and left SP and right SP of animal M2.

To visualize the retained model terms, we treated their coefficients as vectors (Farshadmanesh et al. 2012). The magnitude and direction of the torsional component of these vectors are shown in Fig. 4. White and black bars represent animal M1 and M2 data, respectively. Vectors are shown according to the right-hand rule, so a coefficient with a positive sign means that EMG activity increased with CW orientations/rotations (CW is positive in our coordinate system) and decreased with CCW orientations/rotations (CCW is negative in our coordinate system). This convention was opposite for a negative coefficient. Empty panel (Fig. 4*H*) indicates that no term was retained in the simplified model of right BC in any of the animals.

Table 1. *Corrective movements of pooled left and right INC data: retained terms of simplified models*

	Left Neck Muscles	Right Neck Muscles
	Animal M1	
RCPmaj	$\dot{T}$ (0.36)	$\dot{T}$ (0.29)
OCI	$\dot{T}$ (0.27)	T (0.25)
COM	$\dot{T}$ (0.18)	T (0.11), $\dot{T}$ (0.06)
BC	$\dot{T}$ (0.22), $\ddot{T}$ (0.15)	
SP	$\dot{T}$ (0.24)	$\dot{T}$ (0.20)
SCM	$\dot{T}^2$ (0.38), $\dot{T}$ (0.33)	$\dot{T}$ (0.40)
	Animal M2	
RCPmaj	$\dot{T}$ (0.39)	$\dot{T}^2$ (0.48), $\dot{T}$ (0.27)
OCI	$\dot{T}$ (0.43), $\dot{T}^2$ (0.23)	$\dot{T}$ (0.41), $\dot{T}^2$ (0.27)
COM	$\dot{T}$ (0.45)	$\dot{T}$ (0.38)
BC		
SP	$\dot{T}$ (0.47), $\ddot{T}$ (0.20)	$\dot{T}$ (0.51), $\ddot{T}$ (0.33)
SCM	$\dot{T}$ (0.58), T (0.51), $\dot{T}^2$ (0.33)	$\dot{T}$ (0.65)

The retained orientation and motion terms of the simplified models for corrective movement data pooled for left and right interstitial nucleus of Cajal (INC). These terms collectively contributed more than 0.05 to the sum of square residuals (R^2_{cv}) of the model (see METHODS). To obtain these terms, we added torsional orientation and motion terms to horizontal and vertical orientation terms derived from our behavioral study (Farshadmanesh et al. 2012). Single- and double-dotted letters represent first and second time-derivatives of torsional head orientation (T), respectively. Terms are shown in the order of their contribution to R^2_{cv}. Nos. in parentheses beside each term represent the variance accounted for by that term. RCPmaj, rectus capitis posterior major; OCI, occipital capitis inferior; COM, complexus; BC, biventer cervicis; SP, splenius capitis; SCM, sternocleidomastoid.

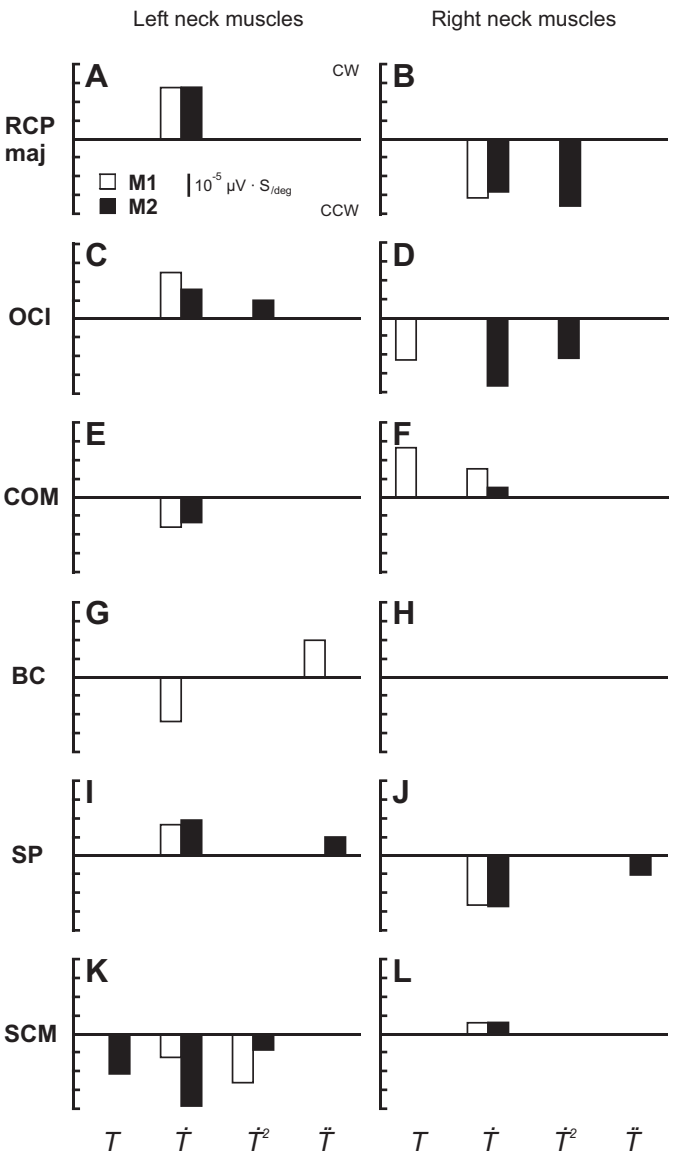

Fig. 4. Coefficients of torsional head orientation (T) and first ($\dot{T}$, $\dot{T}^2$) and second ($\ddot{T}$) time-derivatives of torsional orientation terms of the simplified models. The magnitude (μV·s/°) and direction of the coefficient values are shown for *animals M1* (white bars) and *M2* (black bars). *Left* and *right* columns represent left and right neck muscles, respectively. A positive bar indicates that EMG activity increased with CW orientations/rotations and decreased with CCW orientations/rotations (and vice versa for a negative bar). *A* and *B*: RCPmaj. *C* and *D*: occipital capitis inferior (OCI). *E* and *F*: complexus (COM). *G* and *H*: biventer cervicis (BC). *I* and *J*: splenius capitis (SP). *K* and *L*: sternocleidomastoid (SCM). Empty panel (*H*) indicates that there was no term in the simplified model of right BC in any of the animals.

In both animals, left RCPmaj (Fig. 4*A*) and left OCI (Fig. 4*C*) showed higher activity for CW direction whereas right RCPmaj (Fig. 4*B*) and right OCI (Fig. 4*D*) were more active for CCW direction. Left COM (Fig. 4*E*) and left BC (Fig. 4*G*)

in both subjects showed higher activity for CCW direction with the exception of first-order second time-derivative term ($\ddot{T}$) in animal M1, which showed directionality for CW direction. Right COM (Fig. 4*F*) in both animals was more active for CW direction. Left SP (Fig. 4*I*) and right SP (Fig. 4*J*) in both subjects showed selective activation for CW and CCW directions, respectively. Similarly, in both animals, an opposite activation was observed in bilateral SCM muscles: higher activity in left SCM (Fig. 4*K*) and right SCM (Fig. 4*L*) muscles for CCW and CW directions, respectively. In summary, bilateral neck muscles in both animals showed opposite activation patterns for torsional head movements, consistent with our laboratory's previous results during normal gaze behavior (Farshadmanesh et al. 2012).

Left and Right INC Fits for Stimulation, Corrective, and Inactivation Data Sets

At the next stage of our analysis we derived fits for all six torsional data sets: left vs. right INC for stimulation, corrective and inactivation. We kept the left and right INC populations separate because *1*) for the stimulation and inactivation data these represent fundamentally different brain perturbations; and *2*) we wanted to compare fits derived from left and right INC data. Therefore, for these reasons, we also treated the corrective data the same way for comparison.

The performance of these fits is shown in Fig. 5. This figure shows the R^2_{cv} values averaged across all muscles of each animal, but shown separately for INC stimulation, corrective movement and INC inactivation data sets. White and black bars denote left and right INC data, respectively. For corrective data (Fig. 5, *C* and *D*), the results were comparable to those of the pooled corrective data. In animal M1 (Fig. 5*C*), R^2_{cv} values for left and right INC data were 0.27 and 0.25, respectively, compared with 0.30. Similarly, in animal M2 (Fig. 5*D*), left and right INC results were 0.46 and 0.36 compared with 0.48. For INC stimulation data of animal M1 (Fig. 5*A*), the R^2_{cv} value of left INC data (white bar) was similar to that of corrective data shown in Fig. 5*C* (0.27 vs. 0.27). The model performance for right INC data, however, was higher for stimulation data compared with corrective data (0.33 vs. 0.25). In animal M2, these values were 0.37 vs. 0.46 for left INC and 0.40 vs. 0.36 for right INC. For INC inactivation data of animal M1 (Fig. 5*E*), the R^2_{cv} was lower for left INC compared with corrective data (0.23 vs. 0.27), whereas the values for right INC were similar (0.25 vs. 0.25). In animal M2 (Fig. 5*F*), R^2_{cv} values were lower for left (0.41 vs. 0.46) and higher for right (0.46 vs. 0.36) INC compared with corrective data shown in Fig. 5*D*.

The terms of the simplified models for INC stimulation, corrective movement, and INC inactivation data sets are shown in Tables 2–4, respectively. Several trends are visible in both animals. Overall, more orientation terms were retained in INC inactivation data set compared with other two conditions, with the latter two being less consistent between muscles within and across subjects. Motion terms, however, were retained in 11 (M1) and 10 (M2) muscles during corrective movements, 6 (M1) and 7 (M2) muscles (mostly larger ones, e.g., SP and SCM) during INC stimulation, and only 3 (M1) and 4 (M2) muscles during INC inactivation. But again, the distribution of torsional orientation was relatively restricted in our stimulation data set (Fig. 2*F*), and the distribution of velocity and acceleration terms were relatively restricted in our inactivation data set (Fig. 3, *H* and *L*). This suggests that, when terms appeared in one or two conditions but not the other(s), this likely coincided with different kinematic distributions in the data. This notion is further illustrated and quantified in the regression analyses below.

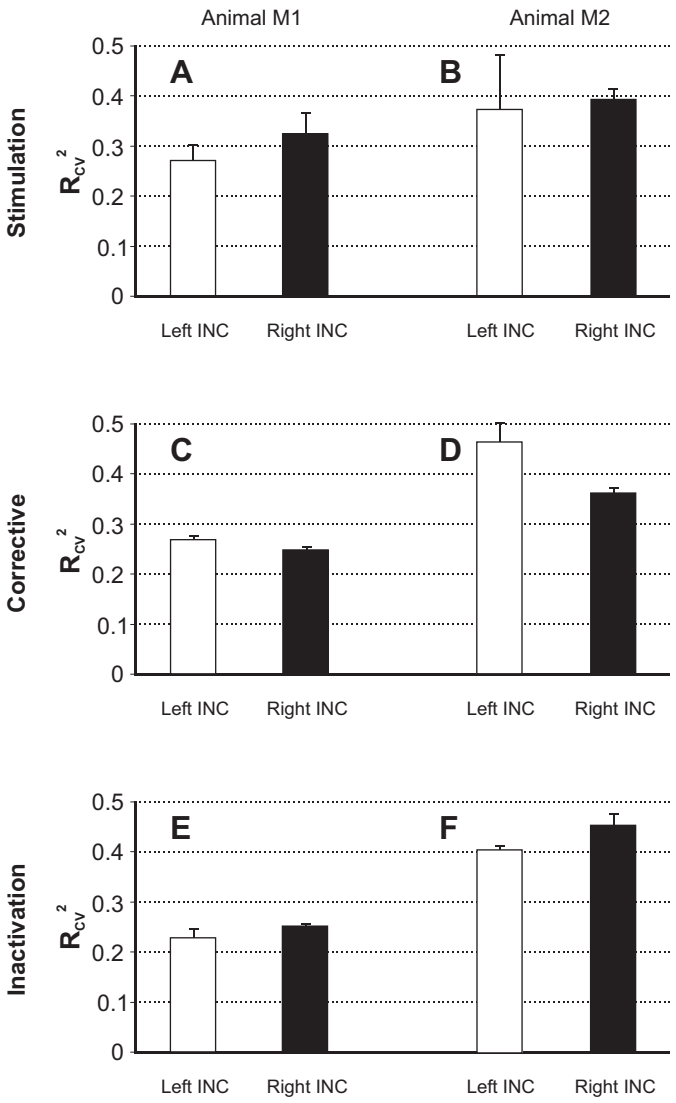

Fig. 5. Sum of square residuals (R^2_{cv}) results of INC stimulation (*A* and *B*), corrective movement (*C* and *D*), and INC inactivation (*E* and *F*) data for *animals M1* (*left* column) and *M2* (*right* column). The R^2_{cv} values for all muscles were pooled and averaged within each animal. Error bars denote standard error.

Comparative Analysis

The final goal of our analysis was to directly compare fits derived from our various data sets to *1*) establish muscle synergies; *2*) determine physiological and anatomic symmetry; *3*) determine how the fits were limited by data set distributions; and *4*) determine whether or not EMG-kinematic coupling is intrinsic to muscle properties, or is it also influenced by the type of neural drive, i.e., in this experiment, stimulation vs. corrective vs. inactivation data. Below, we will compare our results in several ways to examine the effect of different experimental conditions on the relationship between neck

Table 2. *INC stimulation data: retained terms of simplified models*

	Left Neck Muscles	Right Neck Muscles
	Animal M1, left INC	
RCPmaj		
OCI		$\dot{T}$ (0.20)
COM		
BC		
SP	$\dot{T}$ (0.28), $\ddot{T}$ (0.18), T^2 (0.07)	$\dot{T}$ (0.25), $\dot{T}^2$ (0.20), $\ddot{T}$ (0.11)
SCM	$\dot{T}$ (0.36), $\ddot{T}$ (0.21)	$\dot{T}$ (0.22)
	Animal M1, right INC	
RCPmaj	T (0.21)	$\dot{T}^2$ (0.25)
OCI		$\dot{T}T$ (0.23), $\dot{T}$ (0.15)
COM		
BC		
SP	$\dot{T}$ (0.33), $\ddot{T}$ (0.25)	$\dot{T}$ (0.30), T (0.16), $\ddot{T}$ (0.09)
SCM	$\dot{T}$ (0.38)	$\dot{T}$ (0.25), $\dot{T}^2$ (0.20), $\ddot{T}$ (0.13)
	Animal M2, left INC	
RCPmaj	$\dot{T}$ (0.35)	
OCI	$\dot{T}^2$ (0.19)	
COM		
BC		
SP	$\dot{T}$ (0.43), $\dot{T}^2$ (0.17)	$\dot{T}$ (0.25), $\ddot{T}$ (0.22)
SCM	$\dot{T}$ (0.39), $\ddot{T}$ (0.29)	T (0.28), $\dot{T}$ (0.22), $\ddot{T}$ (0.20)
	Animal M2, right INC	
RCPmaj		
OCI	$\dot{T}$ (0.28), T (0.16), $\dot{T}^2$ (0.12)	
COM	$\dot{T}T^2$ (0.15)	T^2 (0.10)
BC		
SP	$\dot{T}^2$ (0.20)	$\dot{T}$ (0.29), T (0.14)
SCM	$\dot{T}$ (0.35), $\dot{T}^2$ (0.30), $\ddot{T}$ (0.22)	$\dot{T}$ (0.37), $\ddot{T}$ (0.21)

The retained orientation and motion terms of the simplified models for INC stimulation data. Conventions are the same as in Table 1.

EMG and head kinematics. To do this, we chose the most consistently retained terms, i.e., which we defined as those that appeared at least six times in all data sets in both animals. Therefore, based on this criterion, we only used the first-order terms (T, $\dot{T}$, $\ddot{T}$) to generate the next three figures (terms of which enough numbers survived our model simplification to allow the comparison). Figures 6–8 plot the regressions we used to compare similar terms (black, T; red, $\dot{T}$; blue, $\ddot{T}$) between different pairings of our six data sets for both M1 (*left* column) and M2 (*right* column). Absent parameters are represented on the graphic plots as zero (unfilled symbols) and were not included in regression fits (the absence of a parameter does not mean it equals zero, it only means it did not survive significance in our cross-validation procedure, in some cases because of limited data). Shaded quadrants (*top-right* and *bottom-left*) indicate the expected distributions of data for a positive correlation; unshaded, for negative correlation.

Anatomic and Neural Symmetry

Right vs. left neck muscles. Here, we tested the expectation that right vs. left muscle pair activation should show opposite kinematic coupling for the same premotor activation patterns, predicting negative correlations in their fit terms. In Fig. 6, the coefficient values of the models of right neck muscles are plotted along the *y*-axis as a function of the corresponding terms for left neck muscles (*x*-axis) for both left and right INC data sets. *Rows 1–3* show the results for INC stimulation (*first* row; *A* and *B*), corrective movements (*middle* row; *C* and *D*), and INC inactivation (*third* row; *E* and *F*) data sets. In this comparison between different muscles, we cannot account for muscle-to-muscle differences in our parameter normalization procedure, so precise quantitative predictions are not possible. Nevertheless, a clear pattern emerged.

For shared terms, the data distributions fell within the unshaded quadrants, as expected for an opposite kinematic coupling for left and right muscle pairs. During INC stimulation (Fig. 6, *A* and *B*), where only velocity (red) and acceleration (blue) terms were retained in both members of some muscle pairs, these showed a negative correlation between bilateral neck muscles [M1 slope = -0.67 ± 0.30 (95% confidence interval, with the slope of -1 suggesting symmetry), $r = -0.97$, $P = 0.0017$; M2 slope = -0.76 ± 0.26, $r = -0.77$, $p = 0.13$]. In corrective movements (Fig. 6, *C* and *D*), where more terms (including some orientation terms) survived in members of more muscle pairs, this negative correlation was significant in both animals (M1 slope = -0.65 ± 0.13, $r = -0.89$, $P = 0.00027$; M2 slope = -0.68 ± 0.19, $r = -0.87$, $P = 0.0044$). The relationship also showed a negative correlation in the inactivation data, where only orientation terms (black) survived (M1 slope = -1.12 ± 0.27, $r = -0.92$, $P = 0.25$; M2 slope = -0.80 ± 0.17, $r = -0.77$, $P = 0.041$). In summary, out of these three comparisons in both animals, there was a negative correlation (significant in four out of six cases),

Table 3. *Corrective movement data: retained terms of simplified models*

	Left Neck Muscles	Right Neck Muscles
	Animal M1, left INC	
RCPmaj	$\dot{T}$ (0.26)	$\dot{T}$ (0.35), $\dot{T}^2$ (0.26)
OCI	T (0.18), $\dot{T}$ (0.13)	$\dot{T}$ (0.21), T (0.16)
COM	$\dot{T}$ (0.25)	T (0.17)
BC	T^2 (0.11)	T (0.16), $\dot{T}$ (0.12), T^2 (0.08)
SP	$\dot{T}$ (0.24)	$\dot{T}$ (0.26)
SCM	$\dot{T}$ (0.33)	$\dot{T}$ (0.21)
	Animal M1, right INC	
RCPmaj	$\dot{T}$ (0.29)	$\dot{T}$ (0.27), T (0.22), $\dot{T}^2$ (0.12)
OCI	$\dot{T}$ (0.18)	T (0.21), T^2 (0.16)
COM	T (0.25)	T (0.20)
BC	$\dot{T}$ (0.15), T (0.09)	$\dot{T}$ (0.15)
SP	$\dot{T}$ (0.22)	$\dot{T}$ (0.26)
SCM	$\dot{T}$ (0.30)	$\dot{T}$ (0.35), $\dot{T}^2$ (0.21)
	Animal M2, left INC	
RCPmaj	$\dot{T}$ (0.42), $\ddot{T}^2T$ (0.28)	$\dot{T}$ (0.50), $\dot{T}^2$ (0.26)
OCI	$\dot{T}$ (0.29), T (0.20), $\dot{T}^2$ (0.16)	$\dot{T}$ (0.26), $\dot{T}^2$ (0.20), T^2 (0.11)
COM	$\dot{T}$ (0.33), $\dot{T}^2$ (0.17)	T (0.19)
BC		
SP	$\dot{T}$ (0.44), $\dot{T}^2$ (0.22)	$\dot{T}$ (0.45), $\ddot{T}$ (0.20)
SCM	$\dot{T}$ (0.51), T (0.35)	$\dot{T}$ (0.46), $\ddot{T}$ (0.27)
	Animal M2, right INC	
RCPmaj	$\dot{T}$ (0.29)	$\dot{T}$ (0.34)
OCI	$\dot{T}^2$ (0.31), T (0.19)	$\dot{T}$ (0.36), $\dot{T}^2$ (0.26), $\ddot{T}^2T$ (0.15)
COM	$\dot{T}$ (0.30),$\ddot{T}$ (0.21)	T (0.22), $\dot{T}$ (0.17)
BC		
SP	$\dot{T}$ (0.27)	T (0.21), $\dot{T}$ (0.16), $\ddot{T}$ (0.10)
SCM	$\dot{T}$ (0.38)	$\dot{T}$ (0.33)

The retained orientation and motion terms of the simplified models for corrective movement data (separate for left and right INC). Conventions are the same as in Table 1.

Table 4. *INC inactivation data: retained terms of simplified models*

	Left Neck Muscles	Right Neck Muscles
	Animal M1, left INC	
RCPmaj		T (0.25), $\dot{T}^2$ (0.18)
OCI	$\dot{T}$ (0.19), T^2 (0.15), T (0.08)	
COM		T (0.21)
BC		T (0.18)
SP	$\dot{T}$ (0.17)	T (0.20), T^3 (0.16), T^2 (0.11)
SCM	T (0.24)	
	Animal M1, right INC	
RCPmaj		T (0.28)
OCI	T (0.22), $\dot{T}$ (0.16), T^2 (0.12)	T (0.21)
COM		
BC		
SP	$\dot{T}$ (0.19), T (0.15)	T (0.18)
SCM	T^2 (0.25), T (0.20)	$\dot{T}$ (0.20), T (0.14)
	Animal M2, left INC	
RCPmaj		T^2 (0.30)
OCI	T (0.37)	
COM	T (0.35)	T (0.29)
BC		
SP	T^2 (0.33), T (0.27)	T (0.38)
SCM	$\ddot{T}$ (0.25), T (0.20)	T (0.37)
	Animal M2, right INC	
RCPmaj	$\dot{T}$ (0.31), T^2 (0.25)	
OCI	$\dot{T}^2$ (0.26), T (0.20), T^2 (0.14)	T (0.42)
COM	T (0.38)	
BC		
SP	T (0.39)	T (0.40)
SCM	T (0.44), T^2 (0.39)	T^2 (0.40), T (0.31), $\dot{T}$ (0.18)

The retained orientation and motion terms of the simplified models for INC inactivation data. Conventions are the same as in Table 1.

the slope was always negative, and its confidence interval never contained zero.

Right vs. left INC. Here, we tested whether the directional source of input to the muscles, e.g., left INC vs. right INC, influences EMG-kinematic coupling. At first glance, one might expect a negative correlation (because the direction of movement is opposite), but note that we are not deriving neural-kinematic coupling or neuromuscular coupling; we are deriving muscle activation-kinematic coupling. If this coupling is independent of the input, the corresponding terms from left vs. right fits should be positively correlated, i.e., appear in the shaded quadrants of Fig. 7. This is expected if, for example, muscles are activated successively more for successively more CW rotation (a positive term), and successively less for successively more CCW orientation (also a positive term), or vice versa. Here, we are making comparisons within muscles over comparable (but opposite) kinematic ranges, so high correlations and a slope of one can be expected if EMG-kinematic coupling is fixed.

Figure 7 plots the surviving T, $\dot{T}$, and $\ddot{T}$ terms as in Fig. 7, but this time for right vs. left INC data during stimulation (*upper* row), correction (*middle* row), and inactivation (*lower* row) conditions. The terms for left and right neck muscle pairs are plotted separately within the same panels. This time, each and every shared term in every animal and condition appeared in the shaded quadrants. This gave rise to a positive correlation between left and right INC data for all conditions and both animals: stimulation [M1 slope = 0.95 ± 0.30 (95% confidence interval), r = 0.99, P = 0.00014; M2 slope = 1.27 ± 0.26, r = 0.99, P = 0.00020], corrective [M1 slope = 1.03 ± 0.14, r = 0.97, P = 0.00000058; M2 slope = 0.97 ± 0.13, r = 0.98, P = 0.0000000086], and inactivation [M1 slope = 0.90 ± 0.17, r = 0.90, P = 0.0059; M2 slope = 0.96 ± 0.20, r = 0.93, P = 0.0074]. This suggests that even though left and right INC stimulation/correction/inactivation evoked opposite behaviors (i.e., CW vs. CCW), individual neck muscles still made a similar contribution to head kinematics through increased or decreased activation. In summary, of the three comparisons done in both animals, correlation (r) was 0.90–0.99 and highly significant, and the confidence interval for the slope always contained 1.0 (except in one marginal case off by 0.01).

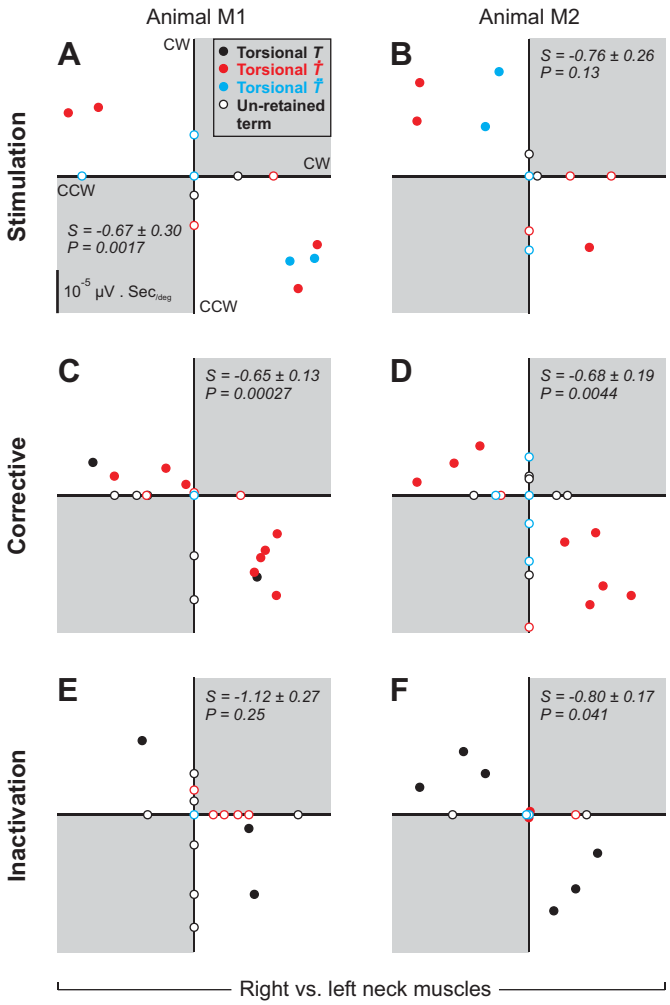

Fig. 6. The magnitude (μV·s/°) of model term coefficients shown for right vs. left neck muscles. Data are shown for INC stimulation (*first* row; *A* and *D*), corrective movements (*middle* row; *B* and *E*), and inactivation (*third* row; *C* and *F*) data. *Left* and *right* columns represent data for *animals M1* and *M2*, respectively. Black dots: torsional head orientation (T); red dots: first time-derivatives of torsional head orientation ($\dot{T}$); blue dots: second time-derivatives of torsional head orientation ($\ddot{T}$). Filled symbols represent the data that were included in the statistical analysis. Unfilled symbols denote the terms that were absent for one of the groups being compared (e.g., here, right vs. left neck muscles) and were excluded from the statistical analysis. Shaded quadrants (*top-right* and *bottom-left*) indicate the expected distributions of data for a positive correlation; unshaded for negative correlation. Vertical scale bar in the *bottom* of *A* denote 10^{-5} μV·s/°. S denotes the slope of the fitted line (95% confidence interval).

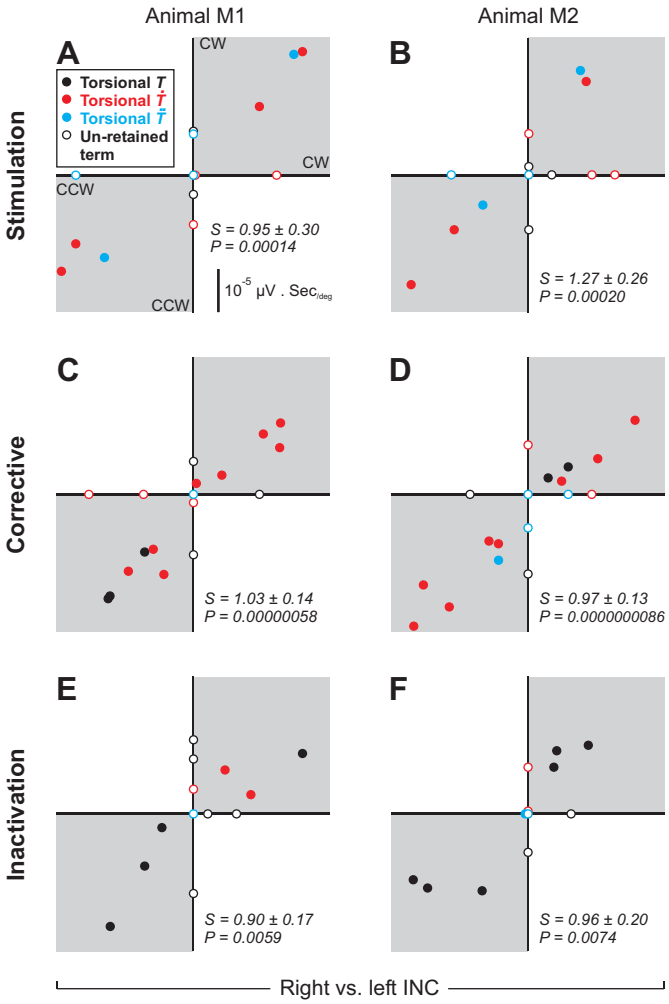

Fig. 7. The magnitude (μV·s/°) of model term coefficients shown for right vs. left neck INCs. Data are shown for INC stimulation (*first* row; *A* and *B*), corrective movements (*middle* row; *C* and *D*), and INC inactivation (*third* row; *E* and *F*) data. Plotting conventions are the same as in Fig. 6.

Influence of Perturbation Source on EMG-Kinematic Coupling

In the remaining plot, we compare our three different data sets to determine whether our model fits were independent of the nature of the premotor perturbation and whether any differences could be accounted for by differences in the kinematic distributions (in which case one would expect certain terms to be missing, but the remaining terms to correlate positively). To summarize, this appears to be the case: the unshared terms appear to result from differences in data distributions, and as for the shared terms, every single pair in every animal and every comparison fell within the gray shaded areas of Fig. 8. Here, we are making comparisons within muscles but different kinematic ranges. The following provides a more detailed description.

INC stimulation vs. corrective movements. Figure 8, *A* and *B*, plots model term coefficients of INC stimulation as a function of those of corrective movement data. Based on their kinematic distributions alone (see Figs. 2 and 3), one might expect fewer orientation terms to appear in the stimulation data set as opposed to the corrective data set. Indeed, in both animals, orientation terms (black dots) were retained more during corrective movements. This is seen by black dots scattered along the *x*-axis with little spread along the *y*-axis (except for two dot in animal M1 and three in animal M2). First time-derivative terms (red dots) were either scattered along the *x*-axis or showed a positive correlation between the two conditions. Finally, second time-derivative terms (blue dots) were retained more in stimulation data compared with corrective movement data (i.e., blue dots were mostly scattered along the *y*-axis). Despite these differences in parameter retention, the stimulation and corrective conditions shared several parameters across muscles, mainly torsional velocity (red), but also torsional orientation (black) and acceleration (blue) terms, each for two muscles in M2. In every case of the shared terms, the paired comparison fell within the gray quadrants, overall yielding positive correlations [M1 slope = 1.40 ± 0.18 (95% confidence interval), r = 0.90, P = 0.00034; M2 slope = 1.05 ± 0.14, r = 0.89, P = 0.000089].

INC inactivation vs. corrective movements. Figure 8, *C* and *D*, represents model term coefficients of INC inactivation data plotted as a function of those of corrective movement data. Based on their kinematic distributions alone (Figs. 2 and 3), one might expect fewer motion (i.e., orientation time-deriva-

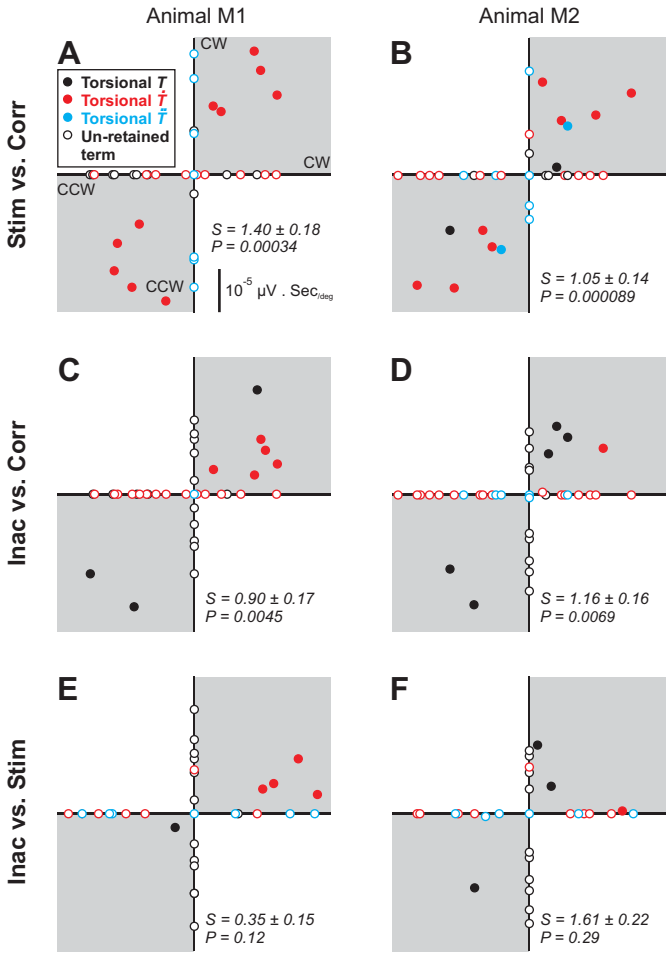

Fig. 8. The magnitude (μV·s/°) of model term coefficients shown for INC stimulation vs. corrective movement (*first* row; *A* and *B*), INC inactivation vs. corrective movement (*middle* row; *C* and *D*), and INC stimulation vs. INC inactivation (*third* row; *E* and *F*) data. Plotting conventions are the same as in Fig. 6.

tive) terms in the inactivation data compared with the corrective data. In both animals, more orientation terms (black dots) were retained during INC inactivation (i.e., along the *y*-axis), whereas first time-derivative terms (red dots) were more common in corrective movement data (i.e., along the *x*-axis). Except for one INC site in animal M1 (Fig. 8*C*, blue dot), second time-derivative terms were only retained in corrective movement data of animal M2 (Fig. 8*D*, blue dots along the *x*-axis). However, in both animals, in cases where orientation and velocity terms were retained during both inactivation and corrective movement conditions, every pairing fell within the gray quadrants, yielding positive correlations [M1 slope = 0.90 ± 0.17 (95% confidence interval), $r = 0.87$, $P = 0.0045$; M2 slope = 1.16 ± 0.16, $r = 0.89$, $P = 0.0069$].

INC inactivation vs. INC stimulation. Figure 8, *E* and *F*, shows INC inactivation vs. INC stimulation coefficients. In this case, based on their kinematic distributions alone (Figs. 2 and 3), one would expect inactivation fits to have more orientation terms while stimulation fits to have more motion terms. Indeed, orientation terms in both animals were retained more during INC inactivation compared with INC stimulation (i.e., along the *y*-axis). This was opposite for both first and second time-derivative terms which were more common during INC stimulation (i.e., along the *x*-axis). Therefore, not surprisingly, this comparison yielded the fewest shared terms (only four velocity and one orientation terms in M1 and three orientation terms in M2). Nevertheless, these terms all fell within the gray quadrants and yielded positive correlations [M1 slope = 0.35 ± 0.15 (95% confidence interval), $r = 0.78$, $P = 0.12$; M2 slope = 1.61 ± 0.22, $r = 0.90$, $P = 0.29$].

In summary, the latter three comparisons in Fig. 8 show that *1*) the presence or absence of most of EMG-kinematic terms could be predicted from the kinematic distribution of our data set; and *2*) those terms that were retained across both data sets in each compared pair always showed a significant positive correlation and above the zero range (in three of six cases containing 1.0), suggesting that the EMG-kinematic coupling is quite consistent across conditions.

DISCUSSION

The present study is the first to examine neck EMG across a large range of torsional head kinematics using a cross-validation-based stepwise regression technique. In a previous study (Farshadmanesh et al. 2012), we used this approach to study the relationships between neck EMG and head kinematics during natural head movements. But due to the much smaller variance in torsional relative to horizontal and vertical kinematics, we could not establish a reliable relationship between neck EMG and head torsion. Here we used stimulation and inactivation of the INC, a brain stem structure thought to control head torsion (Fukushima 1987; Klier and Crawford 2003; Klier et al. 2002), to obtain a large range of torsional head orientations and rotations in monkeys. This provided us with three data sets to test the coupling between EMG in the same six neck muscle pairs tested before and torsional head kinematics: INC stimulation, corrective poststimulation movements, and INC inactivation data sets. To focus our analysis and complete our 3D model, we used the horizontal and vertical kinematic terms derived from our previous study and only allowed the torsional terms to vary (note that the horizontal and vertical ranges here were similar to that paper, see METHODS). We did this for practical purposes, i.e., because this analysis is computationally intensive and required a great amount of processing resources. The present study suggests that such terms hold up well across different data sets. However, it is theoretically possible that some horizontal and vertical terms retained in our previous analysis would no longer be retained in the new data sets, i.e., if all 70 possible terms were allowed to vary. But even if this proved true, these terms would still be required to describe the combined data sets from both studies. Therefore, we chose to focus on torsional terms in the present study, and we believe that the combination of terms from these two studies to be a good approximation of a complete model for the system in these behavioral conditions. Finally, based on the coupling terms we found, and several simplifying principles, it should be possible to infer levels of EMG activation from head kinematics and thus the neural inputs required to produce such patterns of activation.

To summarize our main findings, the corrective torsional movement data set employed here yielded somewhat better cross-validated results (R^2_{cv}) compared with our previous natural head movement data set (M1, 0.30 vs. 0.25; M2, 0.48 vs. 0.36). Similar to our laboratory's previous study, we did not find a significant difference between Fick and space coordinate systems. Our comparison between the three tested data sets suggests that most of observed EMG-kinematic terms could be predicted from the kinematic distribution of examined data sets. During all conditions, bilateral muscle pairs showed similar but opposite kinematic coupling, meaning that for a given value of any one kinematic variable, recruitment on one side was associated with decreased recruitment on the other. However, when the terms for any one muscle were compared across different conditions (stimulation, inactivation, correction, left vs. right INC), the relationship between muscle activation and torsional kinematics always yielded a positive correlation and often slopes near one. This suggests that torsional EMG-kinematic coupling is invariant to different inputs and movement directions. The implications of these findings are explored in more detail below.

Neck Muscle Contributions During Natural vs. Torsionally-Perturbed Head Rotations

In our laboratory's previous study of neck EMG during natural gaze shifts (Farshadmanesh et al. 2012), we did not find a clear relationship between neck EMG and head torsion during static head posture (i.e., none of the tested muscles had a torsional orientation term in their simplified model). During head movements, we observed torsional directionality in RCPmaj, OCI, SP, and SCM, similar to previous findings in monkeys (Farshadmanesh et al. 2008) and humans (Conley et al. 1995). We did not find a relationship between the EMG activity in neck extensors (COM and BC) and head torsion. During the acceleration phase of the observed head movements, the first-order first head orientation time-derivative term ($\dot{T}$) was retained mostly in models for bilateral RCPmaj and OCI in both animals, bilateral SP and SCM in animal M1, and right SP in M2 and none of the neck extensor muscles. First-order second head orientation time-derivative term ($\ddot{T}$) or its interaction with torsional orientation terms were observed in a few muscles and were inconsistent between bilateral muscles

and across animals. However, we concluded that this was largely due to limitations in the torsional range of the movements.

Of our three data sets, our corrective head movement data set was deemed to be the closest approximation of natural head movements. This data set provided the best distribution of head kinematics overall and was presumably generated by endogenous circuits. For this data set, most of the tested neck muscles in both animals retained motion terms in their simplified models, whereas head orientation and second time-derivative terms were retained less frequently and less consistently.

Our results here suggest a clear difference between head kinematics during natural head movements and those evoked by INC perturbations, including the corrective head movements (see Figs. 2 and 3), which might imply different requirements related to torsional head rotations. Therefore, it is quite possible that the neck extensors examined here exhibited different recruitment synergies because of the different torsional head kinematics observed here. Moreover, it is important to note that, while the stimulation-evoked movements are center-out, the corrective movements are out-center. Together, these points suggest that these muscles might also show a different activation for head torsion should different task requirements emerge. However, our data predict that the coupling between this activity and the kinematics of head motion would remain consistent in different tasks.

Relationship to Anatomy and 3D Behavior. It is necessary to empirically determine the contributions of neck muscles to head kinematics because the complexity and redundancy of neck muscles do not allow one to assume their kinematic contributions from anatomy. This has also been reported in less redundant musculoskeletal systems (e.g., limb) where one would expect more consistency between muscle activation and anatomy (Kurtzer et al. 2006; Nozaki et al. 2005). Indeed, during normal gaze behavior (Farshadmanesh et al. 2012), our simplified models for static head posture sometimes did not agree with the kinematic contributions that one would predict from the anatomy. For head movements, however, similar to the present study, we found a higher degree of conformity between our parameters and pulling directions based on anatomy. This, at least for torsional head rotations, suggests a somewhat simpler level of organization, which we hoped might reveal the natural coordinate system for 3D muscle control.

The observed behavior during eye-head gaze shifts, the anatomy of cervical spinal column (Richmond and Vidal 1998), and brain stem control signals (Klier et al. 2007) all suggest a potential contribution of neck muscles to a Fick strategy, similar to that of eye muscles to Listing's law (Demer et al. 1995; Klier et al. 2006; Meng et al. 2005). In our laboratory's previous study of natural head movements (Farshadmanesh et al. 2012), we proposed that performing our analysis on data with a larger range of torsional head kinematics might provide enough variance to discriminate different coordinate systems. Here, while our three data sets provided a substantially larger range of torsional head kinematics (see Figs. 2 and 3), our cross-validated results were still not significantly different for space and Fick coordinates. Thus, unfortunately, our data do not address coordinate systems or muscular contribution to the Fick constraint.

Effect of the Kinematic Range on Deriving Model Terms

In this study, all of our three tested data sets had different kinematic distributions. For torsional head orientation (Fig. 2), all three data sets had a larger distribution compared with control data with corrective movement and INC inactivation data sets showing a broader distribution compared with INC stimulation data set. As expected from the evoked behavior, INC inactivation distributions were shifted in opposite directions compared with INC stimulation and corrective movement data. For head orientation time-derivatives (i.e., head velocity and acceleration), while the ranges for INC perturbation data sets were similar to that of control data (see Fig. 3), they were shifted in opposite directions for INC stimulation and corrective movement data, providing a broader range for time-derivatives. The distribution for INC inactivation data, however, was centered around zero torsion, similar to control data.

These different ranges of head kinematics, both across the different perturbations and relative to the control data, were also observed in the retained terms of our simplified models for each data set. Conversely, when common terms were retained in more than one data set, these corresponded to common kinematic ranges. This suggests that the presence of terms in our cross-validation procedure is more instructive than their absence. Only by combining these three data sets and comparing across them (see below) could we derive and confirm a complete model.

Implications for Internal Models of Head Control

One of the most influential theories in motor control is that the brain uses "internal models" of the mechanical properties of the control system (Flanagan and Wing 1997; Kawato and Wolpert 1998). In particular, it might use "inverse" models to convert desired kinematic states into commands for the levels of muscle activity necessary to achieve those states (Shadmehr and Wise 2005). This requires a detailed internal "knowledge" of the muscles and skeletomotor system. One example is the notion that the INC forms part of something similar to a "neural integrator" that controls 3D orientation of the head (Farshadmanesh et al. 2007; Klier et al. 2002; Klier et al. 2007). This is only possible if the output of the INC is transformed into the appropriate muscle commands to achieve that head orientation.

The EMG-kinematic coupling terms derived in this study, and our laboratory's previous study (Farshadmanesh et al. 2012) do not directly indicate neural inputs, but rather they tell us something about the type of muscle inputs required to achieve certain kinematic variables. This is exactly the type of information required in an inverse kinematic model. Our data are still not complete: one needs to account for head translations as well, all head behaviors, all muscles, and additional knowledge about the transfer functions between motoneuron input and EMG activity. However, they provide the EMG-kinematic terms for rotations in six muscle pairs, at least across the gaze behaviors we tested. This provides a number of the parameters for an internal model of head control and also reveals several other principles.

First, in this study we found that, wherever torsional terms were retained, they were very similar, regardless of how we tested the system, i.e., INC stimulation vs. corrective movements, vs. INC inactivation, and left INC data vs. right INC

data (accounting for the limits in the data range discussed in the preceding section). At first glance it might seem odd that the same muscle would have the same EMG-kinematic coupling during, e.g., CW head tilt and CCW head tilt, but this simply means that *1*) it shows suppressed activity for one direction and increased activity for the other direction, and *2*) the same relationship holds for smaller variations that occur within the CW and CCW ranges that we obtained. This invariance across behaviors supports the notion that EMG-kinematic coupling is indeed largely an intrinsic property of the mechanical control system. Moreover, it suggests that it may be be possible for the brain to use a single inverse model to control the head during different behaviors. This is a requirement, e.g., for a "neural integrator", to function properly (Klier et al. 2002; Robinson 1989).

Another key observation from this study is that the observed neck muscle recruitment was always lateralized, i.e., increased recruitment of a muscle on one side associated with decreased recruitment of this muscle on the other, for a given change in one of the torsional parameters (orientation, velocity, or acceleration) associated with that muscle. Again, this rule held up, regardless of the experimental condition. Although perhaps not surprising, this laterality provides an important simplifying principle for neural control, by effectively collapsing some of the terms for opposite muscle pairs into one parameter for neural control. For example, this allows for the possibility of a "push-pull" (excitatory-inhibitory) drive like that observed in the oculomotor system (Arnold and Robinson 1997; Robinson 1989). Such a rule makes sense for torsional control, because bilateral muscle pairs tend to work in opposition, and similarly for horizontal turners, but not for vertical turners, which should act in concert to resist gravity. Indeed, we observed bilateral opposition in the horizontal terms, but not the vertical terms of the EMG-kinematic coupling model derived in our laboratory's previous study (Farshadmanesh et al. 2012).

Comparison of Neck Muscle Recruitment Mediated by the Interstitiospinal vs. Tecto-Reticulospinal Systems

Consistent with the previous discussion, lateralized neck muscle recruitment has been observed following unilateral stimulation of the superior colliculus (SC), frontal eye fields (FEF) and supplementary eye fields (SEF) (Chapman et al. 2012; Corneil et al. 2002a; Elsley et al. 2007), and during volitional horizontal head turns in the monkey (Corneil et al. 2001; Lestienne et al. 1995). Cocontraction of neck muscle extensors (e.g., BC or COM) can occur during purely vertical volitional head movements (Corneil et al. 2001), making it likely that the absence of cocontraction observed here is due to the unilateral manipulation of the INC via either stimulation or inactivation. The fact that such lateralized recruitment also occurs following unilateral stimulation of the SC, FEF, and SEF again suggests that descending pathways may be converging on a common circuit, or "inverse model". Whether the circuit mediating lateralized neck muscle recruitment resides in the brain stem (as in the oculomotor system) or in the cervical spinal cord (perhaps by homonymous inhibition) remains unclear at this time. However, our laboratory's work on the head "neural integrator" (Farshadmanesh et al. 2007; Klier et al. 2002; Klier et al. 2007) suggests that the intersitiospinal tract would be involved, at least in the transformation of head orientation signals into appropriate neck muscle commands.

Although the lateralization of neck muscle activity following INC manipulation resembles that following stimulation of the SC, FEF, or SEF, the spatial patterning of the muscle synergy is different. Stimulation of the latter structures evokes predominantly horizontal head movements characterized by consistent recruitment of contralateral OCI and RCPmaj for all movements, with additional recruitment of contralateral SP and ipsilateral SCM for progressively larger and faster head turns (Chapman et al. 2012; Corneil et al. 2002a; Elsley et al. 2007). The recruitment of BC and COM is much more variable following stimulation of these structures, and not obviously related to the kinematics of the evoked head movement. In contrast, we observed some recruitment of BC and COM in relation to experimentally induced or volitional torsional head movements (see Tables 1–4). The increased involvement of these extensor muscles following INC manipulation compared with SC, FEF, or SEF manipulation may relate to differences in the muscle synergies contacted by the interstitiospinal vs. tecto-reticulo-spinal pathways, but such speculation awaits anatomical studies like that performed by Shinoda and colleagues on the vestibulospinal system (Sugiuchi et al. 2004). Furthermore, it is not known whether the neck muscle synergies evoked by manipulation of the interstitiospinal system in the monkey arise from direct contact onto neck muscle motoneurons, or are mediated by interneurons within the spinal cord (see Isa and Sasaki 2002 for review).

Finally, it is likely necessary to account for other non-INC structures to explain the range of data that we obtained in some of our experiments, for example, the residual ability to move the head torsionally in the direction mediated by the inactivated INC (e.g., CW following right INC inactivation). This might be due to incomplete inactivation of the INC. However, it is known that several descending pathways are involved in head control besides the intersitiospinal tract (Isa and Sasaki 2002). Thus it is possible that other pathways that bypass the INC are recruited to compensate for unilateral INC inactivation. Similarly, cortical circuits that bypass an inactivated area were proposed to explain the surprisingly small effects of temporary pharmacological inactivation of the SC on head movements, despite substantial effects on gaze shift timing and velocity (Walton et al. 2008). Furthermore, the head contribution to gaze shifts substantially increases after permanent ablation of the FEF, although this compensatory strategy only appears after 1 wk's recovery (van der Steen et al. 1986). Thus different compensatory strategies are likely recruited following either temporary or permanent ablations of oculomotor circuits. But if so, our data suggest that they tapped into the same EMG-kinematic coupling properties, since we obtained the same terms during INC stimulation, INC inactivation, and corrective head movements.

Clinical Application

Spasmodic torticollis (cervical dystonia) is often characterized by involuntary sustained or repetitive neck muscle contractions which cause abnormal head posture and impair the control of head movements (Chan et al. 1991; Jankovic et al. 1991; Marsden and Quinn 1990). While the etiology of torticollis is still unknown, lesions in the midbrain (Halmagyi et al.

1990; Isaac and Cohen 1989; Ohashi et al. 1998; Plant et al. 1989; Walker et al. 1990), basal ganglia (Bhatia and Marsden 1994; Fahn 1988; Marsden et al. 1985) and vestibular system (Bronstein and Rudge 1986) have been suggested to be involved. In particular, lesions in the INC are reported by several studies to cause abnormal head postures similar to those observed in torticollis (Bertrand et al. 1978; Klier et al. 2002; Loher et al. 2004; Malouin and Bedard 1982; Munchau and Bronstein 2001; Vasin et al. 1985). Indeed, the head tilts we observed during our INC perturbation were similar to torticollis symptoms reported in humans (Loher et al. 2004).

As experimental models, both INC stimulation and inactivation have been suggested to be useful in studying torticollis (Farshadmanesh et al. 2007; Klier et al. 2002; Klier et al. 2007). While these different INC perturbations examine different underlying mechanisms for INC dysfunction (e.g., abnormal input to the INC during INC stimulation or its direct damage during INC inactivation), they could not differentiate between them. The fixed EMG-kinematic coupling observed in the present study, however, can help separate these two approaches by providing a predictive tool that could estimate neck EMG from observed head kinematics (assuming this holds under chronic conditions). Moreover, performing a cross-validation-based approach similar to what we used here, on neck EMG and head kinematics recorded in torticollis patients, and comparing the retained model terms to those reported here, could further provide a robust tool to differentiate different INC abnormalities and potential causes for torticollis (e.g., premotor disturbances vs. abnormalities in the muscles themselves). Having developed the method here, in principle, it should not be hard to implement this as diagnostic software and apply to noninvasive surface EMG measurements for comparison across patient populations.

ACKNOWLEDGMENTS

The authors thank Dr. Xiaogang Yan, Saihong Sun, and Tania Admans for contributions.

GRANTS

This project was supported by an operating grant from the Canadian Institutes of Health Research (CIHR) to J. D. Crawford (MOP 13357), a CIHR Group Grant, and infrastructure support from the Canadian Foundation for Innovation and the Ontario Innovation Trust. F. Farshadmanesh was supported by Ontario Graduate Scholarship in Science and Technology (OGSST). B. D. Corneil was supported by a CIHR New Investigator award, a CIHR grant (MOP 64202 and 93796), and a Career Development award from the Human Frontier Science program. J. D. Crawford was supported by a Canada Research Chair.

DISCLOSURES

No conflicts of interest, financial or otherwise, are declared by the author(s).

AUTHOR CONTRIBUTIONS

Author contributions: F.F., B.D.C., and J.D.C. conception and design of research; F.F. and H.W. performed experiments; F.F. analyzed data; F.F., P.A.B., B.D.C., and J.D.C. interpreted results of experiments; F.F. prepared figures; F.F. drafted manuscript; F.F., P.A.B., H.W., B.D.C., and J.D.C. edited and revised manuscript; F.F., B.D.C., and J.D.C. approved final version of manuscript.

REFERENCES

Angelaki DE, Dickman JD. Premotor neurons encode torsional eye velocity during smooth-pursuit eye movements. *J Neurosci* 23: 2971–2979, 2003.

Arnold DB, Robinson DA. The oculomotor integrator: testing of a neural network model. *Exp Brain Res* 113: 57–74, 1997.

Bak MJ, Loeb GE. A pulsed integrator for EMG analysis. *Electroencephalogr Clin Neurophysiol* 47: 738–741, 1979.

Bertrand C, Molina-Negro P, Martinez SN. Combined stereotactic and peripheral surgical approach for spasmodic torticollis. *Appl Neurophysiol* 41: 122–133, 1978.

Bhatia KP, Marsden CD. The behavioural and motor consequences of focal lesions of the basal ganglia in man. *Brain* 117: 859–876, 1994.

Blohm G, Crawford JD. Computations for geometrically accurate visually guided reaching in 3-D space. *J Vis* 7: 4.1–4.22, 2007.

Blohm G, Khan AZ, Ren L, Schreiber KM, Crawford JD. Depth estimation from retinal disparity requires eye and head orientation signals. *J Vis* 8: 3.1–3.23, 2008.

Bronstein AM, Rudge P. Vestibular involvement in spasmodic torticollis. *J Neurol Neurosurg Psychiatry* 49: 290–295, 1986.

Ceylan M, Henriques DY, Tweed DB, Crawford JD. Task-dependent constraints in motor control: pinhole goggles make the head move like an eye. *J Neurosci* 20: 2719–2730, 2000.

Chan J, Brin MF, Fahn S. Idiopathic cervical dystonia: clinical characteristics. *Mov Disord* 6: 119–126, 1991.

Chapman BB, Pace MA, Cushing SL, Corneil BD. Recruitment of a contralateral head turning synergy by stimulation of monkey supplementary eye fields. *J Neurophysiol* 107: 1694–1710, 2012.

Conley MS, Meyer RA, Bloomberg JJ, Feeback DL, Dudley GA. Noninvasive analysis of human neck muscle function. *Spine (Phila Pa 1976)* 20: 2505–2512, 1995.

Corneil BD, Olivier E, Munoz DP. Neck muscle responses to stimulation of monkey superior colliculus. I. Topography and manipulation of stimulation parameters. *J Neurophysiol* 88: 1980–1999, 2002a.

Corneil BD, Olivier E, Munoz DP. Neck muscle responses to stimulation of monkey superior colliculus. II. Gaze shift initiation and volitional head movements. *J Neurophysiol* 88: 2000–2018, 2002b.

Corneil BD, Olivier E, Richmond FJ, Loeb GE, Munoz DP. Neck muscles in the rhesus monkey. II. Electromyographic patterns of activation underlying postures and movements. *J Neurophysiol* 86: 1729–1749, 2001.

Crawford JD. Listing's law: What's all the hubbub? In: *Vision and Action*, edited by Harris L and Jenkin M. New York: Cambridge University Press, 1998, p. 139–162.

Crawford JD, Ceylan MZ, Klier EM, Guitton D. Three-dimensional eye-head coordination during gaze saccades in the primate. *J Neurophysiol* 81: 1760–1782, 1999.

Crawford JD, Henriques DY, Medendorp WP. Three-dimensional transformations for goal-directed action. *Annu Rev Neurosci* 34: 309–331, 2011.

Crawford JD, Martinez-Trujillo JC, Klier EM. Neural control of three-dimensional eye and head movements. *Curr Opin Neurobiol* 13: 655–662, 2003.

Demer JL, Miller JM, Poukens V, Vinters HV, Glasgow BJ. Evidence for fibromuscular pulleys of the recti extraocular muscles. *Invest Ophthalmol Vis Sci* 36: 1125–1136, 1995.

Demer JL, Oh SY, Poukens V. Evidence for active control of rectus extraocular muscle pulleys. *Invest Ophthalmol Vis Sci* 41: 1280–1290, 2000.

Domzal TM, Tutaj A. [Electromyography monitoring in the treatment of torticollis with botulinum toxin]. *Pol Merkur Lekarski* 8: 474–475, 2000.

Elsley JK, Nagy B, Cushing SL, Corneil BD. Widespread presaccadic recruitment of neck muscles by stimulation of the primate frontal eye fields. *J Neurophysiol* 98: 1333–1354, 2007.

Fahn S. Concept and classification of dystonia. *Adv Neurol* 50: 1–8, 1988.

Farshadmanesh F, Byrne P, Keith GP, Wang H, Corneil BD, Crawford JD. Cross-validated models of the relationships between neck muscle electromyography and three-dimensional head kinematics during gaze behavior. *J Neurophysiol* 107: 573–590, 2012.

Farshadmanesh F, Chang P, Wang H, Yan X, Corneil BD, Crawford JD. Neck muscle synergies during stimulation and inactivation of the interstitial nucleus of Cajal (INC). *J Neurophysiol* 100: 1677–1685, 2008.

Farshadmanesh F, Klier EM, Chang P, Wang H, Crawford JD. Three-dimensional eye-head coordination after injection of muscimol into the interstitial nucleus of Cajal (INC). *J Neurophysiol* 97: 2322–2338, 2007.

Flanagan JR, Wing AM. The role of internal models in motion planning and control: evidence from grip force adjustments during movements of hand-held loads. *J Neurosci* 17: 1519–1528, 1997.

Fukushima K. The interstitial nucleus of Cajal and its role in the control of movements of head and eyes. *Prog Neurobiol* 29: 107–192, 1987.

Fukushima K, Takahashi K, Kudo J, Kato M. Interstitial-vestibular interaction in the control of head posture. *Exp Brain Res* 57: 264–270, 1985.

Glenn B, Vilis T. Violations of Listing's law after large eye and head gaze shifts. *J Neurophysiol* 68: 309–318, 1992.

Graf W, de Waele C, Vidal PP. Functional anatomy of the head-neck movement system of quadrupedal and bipedal mammals. *J Anat* 186: 55–74, 1995.

Halmagyi GM, Brandt T, Dieterich M, Curthoys IS, Stark RJ, Hoyt WF. Tonic contraversive ocular tilt reaction due to unilateral meso-diencephalic lesion. *Neurology* 40: 1503–1509, 1990.

Isa T, Sasaki S. Brainstem control of head movements during orienting; organization of the premotor circuits. *Prog Neurobiol* 66: 205–241, 2002.

Isaac K, Cohen JA. Post-traumatic torticollis. *Neurology* 39: 1642–1643, 1989.

Jankovic J, Leder S, Warner D, Schwartz K. Cervical dystonia: clinical findings and associated movement disorders. *Neurology* 41: 1088–1091, 1991.

Kawato M, Wolpert D. Internal models for motor control. *Novartis Found Symp* 218: 291–304; discussion 304–297, 1998.

Klier EM, Crawford JD. Human oculomotor system accounts for 3-D eye orientation in the visual-motor transformation for saccades. *J Neurophysiol* 80: 2274–2294, 1998.

Klier EM, Crawford JD. Neural control of three-dimensional eye and head posture. *Ann N Y Acad Sci* 1004: 122–131, 2003.

Klier EM, Martinez-Trujillo JC, Medendorp WP, Smith MA, Crawford JD. Neural control of 3-D gaze shifts in the primate. *Prog Brain Res* 142: 109–124, 2003.

Klier EM, Meng H, Angelaki DE. Three-dimensional kinematics at the level of the oculomotor plant. *J Neurosci* 26: 2732–2737, 2006.

Klier EM, Wang H, Constantin AG, Crawford JD. Midbrain control of three-dimensional head orientation. *Science* 295: 1314–1316, 2002.

Klier EM, Wang H, Crawford JD. Interstitial nucleus of cajal encodes three-dimensional head orientations in Fick-like coordinates. *J Neurophysiol* 97: 604–617, 2007.

Kurtzer I, Pruszynski JA, Herter TM, Scott SH. Primate upper limb muscles exhibit activity patterns that differ from their anatomical action during a postural task. *J Neurophysiol* 95: 493–504, 2006.

Lestienne FG, Le Goff B, Liverneaux PA. Head movement trajectory in three-dimensional space during orienting behavior toward visual targets in rhesus monkeys. *Exp Brain Res* 102: 393–406, 1995.

Loher TJ, Pohle T, Krauss JK. Functional stereotactic surgery for treatment of cervical dystonia: review of the experience from the lesional era. *Stereotact Funct Neurosurg* 82: 1–13, 2004.

Malouin F, Bedard PJ. Frontal torticollis (head tilt) induced by electrolytic lesion and kainic acid injection in monkeys and cats. *Exp Neurol* 78: 551–560, 1982.

Marsden CD, Obeso JA, Zarranz JJ, Lang AE. The anatomical basis of symptomatic hemidystonia. *Brain* 108: 463–483, 1985.

Marsden CD, Quinn NP. The dystonias. *BMJ* 300: 139–144, 1990.

Martinez-Trujillo JC, Medendorp WP, Wang H, Crawford JD. Frames of reference for eye-head gaze commands in primate supplementary eye fields. *Neuron* 44: 1057–1066, 2004.

Medendorp WP, Smith MA, Tweed DB, Crawford JD. Rotational remapping in human spatial memory during eye and head motion. *J Neurosci* 22: RC196, 2002.

Medendorp WP, van Gisbergen JA, Horstink MW, Gielen CC. Donders' law in torticollis. *J Neurophysiol* 82: 2833–2838, 1999.

Meng H, Green AM, Dickman JD, Angelaki DE. Pursuit-vestibular interactions in brain stem neurons during rotation and translation. *J Neurophysiol* 93: 3418–3433, 2005.

Munchau A, Bronstein AM. Role of the vestibular system in the pathophysiology of spasmodic torticollis. *J Neurol Neurosurg Psychiatry* 71: 285–288, 2001.

Nozaki D, Nakazawa K, Akai M. Muscle activity determined by cosine tuning with a nontrivial preferred direction during isometric force exertion by lower limb. *J Neurophysiol* 93: 2614–2624, 2005.

Ohashi T, Fukushima K, Chin S, Harada T, Yoshida K, Akino M, Matsuda H. Ocular tilt reaction with vertical eye movement palsy caused by localized unilateral midbrain lesion. *J Neuroophthalmol* 18: 40–42, 1998.

Peterson BW, Choi H, Hain T, Keshner E, Peng GC. Dynamic and kinematic strategies for head movement control. *Ann N Y Acad Sci* 942: 381–393, 2001.

Peterson BW, Richmond FJ. *Control of Head Movement*. New York: Oxford University Press, 1988.

Plant GT, Kermode AG, du Boulay EP, McDonald WI. Spasmodic torticollis due to a midbrain lesion in a case of multiple sclerosis. *Mov Disord* 4: 359–362, 1989.

Radau P, Tweed D, Vilis T. Three-dimensional eye, head, and chest orientations after large gaze shifts and the underlying neural strategies. *J Neurophysiol* 72: 2840–2852, 1994.

Ren L, Crawford JD. Coordinate transformations for hand-guided saccades. *Exp Brain Res* 195: 455–465, 2009.

Richmond FJ, Singh K, Corneil BD. Neck muscles in the rhesus monkey. I. Muscle morphometry and histochemistry. *J Neurophysiol* 86: 1717–1728, 2001.

Richmond FJ, Vidal PP. The motor system: joints and muscles of the neck. In: *Control of Head Movement*, edited by Richmond FJ and Peterson BW. New York: Oxford University Press, 1998, p. 1–21.

Robinson DA. Integrating with neurons. *Annu Rev Neurosci* 12: 33–45, 1989.

Robinson DA. A quantitative analysis of extraocular muscle cooperation and squint. *Invest Ophthalmol* 14: 801–825, 1975.

Shadmehr R, Wise SP. The Computational Neurobiology of Reaching And Pointing: A Foundation for Motor Learning. Cambridge, MA: MIT Press, 2005.

Siegmund GP, Blouin JS, Brault JR, Hedenstierna S, Inglis JT. Electromyography of superficial and deep neck muscles during isometric, voluntary, and reflex contractions. *J Biomech Eng* 129: 66–77, 2007.

Simpson JI, Graf W. Eye-muscle geometry and compensatory eye movements in lateral-eyed and frontal-eyed animals. *Ann N Y Acad Sci* 374: 20–30, 1981.

Straumann D, Haslwanter T, Heppreymond MC, Hepp K. Listings law for eye, head and arm movements and their synergistic control. *Exp Brain Res* 86: 209–215, 1991.

Sugiuchi Y, Kakei S, Izawa Y, Shinoda Y. Functional synergies among neck muscles revealed by branching patterns of single long descending motor-tract axons. *Prog Brain Res* 143: 411–421, 2004.

Tweed D. Listing's law for gaze-directing head movements. In: *The Head-neck Sensory Motor System*, edited by Berthoz A, Graf W, and idal PP. New York: Oxford University Press, 1992, p. 85–99.

Tweed D, Cadera W, Vilis T. Computing three-dimensional eye position quaternions and eye velocity from search coil signals. *Vision Res* 30: 97–110, 1990.

van der Steen J, Russell IS, James GO. Effects of unilateral frontal eye-field lesions on eye-head coordination in monkey. *J Neurophysiol* 55: 696–714, 1986.

Van Opstal J, Hepp K, Suzuki Y, Henn V. Role of monkey nucleus reticularis tegmenti pontis in the stabilization of Listing's plane. *J Neurosci* 16: 7284–7296, 1996.

Vasilescu C, Dieckmann G. Electromyographic investigations in torticollis. *Appl Neurophysiol* 38: 153–160, 1975.

Vasin N, Medzhidov MR, Shabalov VA. Stereotaxic destruction of the interstitial nucleus of Cajal on spastic torticollis. *Zh Vopr Neirokhir Im N N Burdenko*: 3–7, 1985.

Walker FO, Walker JM, Matsumoto RR, Bowen WD. Torticollis, midbrain, and sigma receptors. *Mov Disord* 5: 265, 1990.

Walton MM, Bechara B, Gandhi NJ. Effect of reversible inactivation of superior colliculus on head movements. *J Neurophysiol* 99: 2479–2495, 2008.